Fall 2019

Studies of CH Activation in Unsaturated Amides and Esters by Trinuclear Metal Carbonyl Clusters of Osmium

Morteza Maleki

STUDIES OF CH ACTIVATION IN UNSATURATED AMIDES AND ESTERS BY TRINUCLEAR METAL CARBONYL CLUSTERS OF OSMIUM

By

Morteza Maleki

Bachelor of Science

University of Tehran, 2014

Submitted in Partial Fulfillment of the Requirements

For the Degree of Master of Science in

Chemistry

College of Arts and Sciences

University of South Carolina

2019

Accepted by:

Richard D. Adams, Director of Thesis

Aaron K. Vannucci, Reader

Cheryl L. Addy, Vice Provost and Dean of the Graduate School

DEDICATION

To God, my creator and my savior:

The one and only who created me, guided me, and taught me. The one whom I rely on and to whom I shall return.

To My Parents, Amir and Masoumeh:

The most beautiful people in the world, who sacrificed their lives, so I can go to school and become educated, and will always be proud of me.

To my sister, Mahsa:

Who has been the most kind and the most compassionate in the tough times.

To my love, Sahar:

Who has been with me through all the good and tough days, challenges and celebrations.

ACKNOWLEDGEMENTS

I want to appreciate all the help and kindness from Professor Richard D. Adams since when I was his student in CHEM 711. He taught me the basics of cluster and organometallic chemistry, he taught me how to be a good chemist and the most important of all, how to be a good person. This work would not have been possible without guidance, encouragement, and patience from him. I want to thank all my advisory committee members Dr. Aaron Vannucci, Dr. Thomas Makris, and Dr. Esmaiel Jabbari whose suggestions and support made the path much easier for me to progress in my research.

I would like to thank Jennifer Merkel, whose unique kindness and sense of responsibility facilitated my admission to the University of South Carolina, and later on, comforted my pursuit of knowledge in the program. I want to thank Dr. Thomas Bryson whose advice and support made the graduate school much less stressful and more pleasant. I want to thank Dr. Amelia Taylor Perry and Dr. Leslie Lovelace who made me a good teacher and taught me how to teach and learn at the same time. I want to thank Dr. Mark Smith whose quick analysis of crystal structures made the progress of our work much faster. Last but not least, I want to thank all the help, support and kindness from all the group members in Dr. Adams' group: Gaya Elpitiya, Joseph Kiprotich, Jonathan Tedder, Poonam Dhull, Humaiara Akter, Nutan Wakdikar and Meenal Kaushal. Special thanks to Wilson Carter Edenfield for all his work and assistance on this project.

ABSTRACT

The chemistry of the reaction of $Os_3(CO)_{10}(NCCH_3)_2$ with representatives of unsaturated amides and esters, $RCOCHCH_2$ ($R=(CH_3)_2N$, CH_3O) has been investigated. In these reactions, it has been observed that a CH bond on the β-carbon atom is readily activated by triosmium carbonyl clusters. The activation of β-carbon C-H bond in unsaturated amides and esters provides a robust platform for studying multicenter C-H bond transformations and for C-C bond formation via hydrogen shift and CO insertion processes. In this work, proposed mechanistic approaches have been taken in order to better understand and study the relationship between the characterized species. In addition, a few non-identified species have been predicted to exist. Furthermore, recommendations on how this work can be further studied and improved have been made. A series of activated unsaturated amides and esters: $Os_2(CO)_6(\mu\text{-}H)(\mu\text{-}O{=}C(N(CH_3)_2)CHCH)$, **1**, $Os_4(CO)_{12}(\mu\text{-}O{=}C(N(CH_3)_2)CHCH)_2$, **2**, $Os_3(CO)_9(\mu\text{-}O{=}C(N(CH_3)_2)CH_2CHCCHC(N(CH_3)_2){=}O)$, **3**, $Os_3(CO)_8(\mu\text{-}O{=}C(N(CH_3)_2)CHCH)_2$, **4**, $Os_6(CO)_{20}(\mu\text{-}H)(\mu\text{-}O{=}C(N(CH_3)_2)\ CHCH)$, **5**, $HOs_3(CO)_{10}(\mu\text{-}O{=}C(N(CH_3)_2)CHCH)$, **6**, $Os_5(CO)_{15}(\mu\text{-}O{=}C(N(CH_3)_2)CHCH)_2$, **7**, and $Os_3(CO)_9(\mu\text{-}H)(\mu\text{-}O{=}C(OCH_3)CHCH)$, **8**, were synthesized and isolated. They are described in Chapter 1. Each of the new compounds has been characterized by FT-IR, NMR (^1H), mass-spectra and single crystal X-ray diffraction analysis.

TABLE OF CONTENTS

DEDICATION iii

ACKNOWLEDGEMENTS iv

ABSTRACT v

LIST OF FIGURES vii

LIST OF SCHEMES viii

LIST OF TABLES ix

CHAPTER 1 STUDIES OF CH ACTIVATION IN UNSATURATED AMIDES AND ESTERS BY TRINUCLEAR METAL CARBONYL CLUSTERS OF OSMIUM: STUDY, SYNTHESIS AND CHARACTERIZATION 1

1.1 INTRODUCTION 1

1.2 EXPERIMENTAL DETAILS 8

1.3 CRYSTALLOGRAPHIC ANALYSES 12

1.4 RESULTS AND DISCUSSION 13

1.5 SUMMARY AND CONCLUSIONS 32

1.6 REFERENCES 38

LIST OF FIGURES

Figure 1.1 Molecular structures of MA (left) and DMA (right) 3

Figure 1.2 Nylon 6,6 synthesis pathway from Adipic Acid and Hexamethylene Diamine 5

Figure 1.3 Activation of Methyl Acrylate by $Ru_5(\mu_5\text{-}C)(CO)_{15}$ Complex by Adams et al 6

Figure 1.4 Activation of Vinyl Acetate by $Re_2(CO)_8(\mu\text{-}C_6H_5)(\mu\text{-}H)$ Complex by Adams et al 7

Figure 1.5 Proposed structure of **I***, a saturated 48 e species with the formula of $Os_3(CO)_9(\mu\text{-}H)(\mu_3\text{-}O{=}C(N(CH_3)_2)CHCH)$ 17

Figure 1.6 ORTEP diagram of the molecular structure of $Os_2(CO)_6(\mu\text{-}H)(\mu\text{-}O{=}C(N(CH_3)_2)CHCH)$, **1**, showing 30% thermal ellipsoid probability 20

Figure 1.7 ORTEP diagram of the molecular structure of $Os_4(CO)_{12}(\mu\text{-}O{=}C(N(CH_3)_2)CHCH)_2$, **2**, showing 25% thermal ellipsoid probability 21

Figure 1.8 ORTEP diagram of the molecular structure of $Os_3(CO)_9(\mu\text{-}O{=}C(N(CH_3)_2)CH_2CHCCHC(N(CH_3)_2){=}O)$, **3**, showing 25% thermal ellipsoid probability 22

Figure 1.9 ORTEP diagram of the molecular structure of $Os_3(CO)_8(\mu\text{-}O{=}C(N(CH_3)_2)CHCH)_2$, **4**, showing 15% thermal ellipsoid probability 24

Figure 1.10 An ORTEP diagram of the molecular structure of $Os_6(CO)_{20}(\mu\text{-}H)(\mu\text{-}O{=}C(N(CH_3)_2)CHCH)$, **5**, showing 30% thermal ellipsoid probability 25

Figure 1.11 An ORTEP diagram of the molecular structure of $HOs_3(CO)_{10}(\mu\text{-}O{=}C(N(CH_3)_2)CHCH)$, **6**, showing 20% thermal ellipsoid probabilities 26

Figure 1.12 An ORTEP diagram of the molecular structure of $Os_5(CO)_{15}(\mu\text{-}O{=}C(N(CH_3)_2)CHCH)_2$, **7**, showing 30% thermal ellipsoid probability 27

Figure 1.13 An ORTEP drawing of the molecular structure of $Os_3(CO)_9(\mu\text{-}H)(\mu\text{-}O{=}C(OCH_3)CHCH)$, **8** showing 30% thermal ellipsoid probability 31

LIST OF SCHEMES

Scheme 1.1 Structure of seven activated compounds resulted from reactions of $Os_3(CO)_{10}(NCCH_3)_2$ and DMA: **1**, **2**, **3**, **4**, **5**, **6**, and **7** 15

Scheme 1.2 A proposed mechanism of C-H activation of DMA by triosmium carbonyl cluster and formation of **I*** and **6** 18

Scheme 1.3 A proposed scheme for transformation of **6** to **1**.....27

Scheme 1.4 A proposed scheme for transformation of **6** to **3**.....28

Scheme 1.5 A proposed scheme for transformation of **3** to **4**.....29

Scheme 1.6 A proposed scheme for transformation of **6** to **5**.....29

Scheme 1.7 A proposed scheme for transformation of **1** to **2**.....30

Scheme 1.8 A schematic mechanism for synthesis and transformations of **1**, **2**, **3**, **4**, **5**, **6**, and **7**.....34

LIST OF TABLES

Table 1.1 Crystallographic Data for Compounds **1, 2, 3** 35

Table 1.2 Crystallographic Data for Compounds **4, 5, 6** 36

Table 1.3 Crystallographic Data for Compounds **7, 8** 37

CHAPTER 1

STUDIES OF CH ACTIVATION IN UNSATURATED AMIDES AND ESTERS BY TRINUCLEAR METAL CARBONYL CLUSTERS OF OSMIUM: STUDY, SYNTHESIS AND CHARACTERIZATION

1.1 INTRODUCTION

The selective transformation of ubiquitous but unreactive CH bonds to other functional groups has far-reaching practical implications, ranging from more efficient strategies for fine chemical synthesis to the replacement of current petrochemical feedstocks by less expensive and more readily available alkanes. Metal catalyzed C-H bond activation and subsequent addition of the activated species to unsaturated compounds constitute one of the most economical and efficient methods in organic synthesis.

Functionalization of unsaturated compounds into carbonyl-containing molecules is an area of great interest. [1] Transition metal-catalyzed hydroacylation, hydroesterification, hydrocarbamoylation, and hydroarylation processes including an insertion of unsaturated compounds (such as alkenes[2], alkynes[2], or ketones[3]) into activated C-H bond of aldehydes, constitutes one of the most economical and efficient methods for the C-C bond formation. These transformations of simple unsaturated hydrocarbons to compounds with more functional groups are very important and highly valuable in the chemical industry, pharmaceuticals and organic research. It also helps us study and better understand catalytic

systems and solvent systems to be able to propose and predict the result of more reactions in the future.[4]

Condensation polymers such as polyesters and polyamides are of great importance in industrial manufacturing. Nylon is the most prominent polyamide used in industry and has numerous applications such as textiles, automotive industry, carpets, utensils and sportswear due to their high durability and strength. The transportation manufacturing industry is the major consumer, accounting for 35% of polyamide (PA) consumption. In addition, nylon is recyclable and can easily be re-made and re-used through particular industrial processes which makes a carbon efficient feedstock of most polymeric products.

Methyl Acrylate (MA) is one of the most significant esters used predominantly in industry and as a precursor for many of catalytic reactions. Hence, dimerization of methyl acrylate has commanded a lot of attention throughout the years, among which, transition metal catalyzed activation and dimerization or polymerization of this olefin has been the center of attention for a long time. Monometallic and bimetallic clusters of transition metals of Pd, Ru, Pt, and Rh have been successfully utilized, studied, and reported for this purpose. Unlike numerous studies carried out on activation and end to end dimerization of MA, there are not many examples of activation or dimerization of N, N-Dimethylacrylamide (DMA) using transition metals.

As will be mentioned later in this report, Adams et al. have studied activation and functionalization of DMA using $Ru_5(\mu_5\text{-}C)(CO)_{15}$ cluster and characterized the isolated complexes. Figure 1.1 shows the line structure for MA and DMA.

Despite all the effort in order to functionalize DMA using $Ru_5(\mu_5\text{-}C)(CO)_{15}$, end to end dimerization of DMA is unique to this work and there is no reported complex which possesses such configuration of the chelated DMA. Moreover, osmium has not been used to activate either of MA or DMA molecules and study of CH activation in any of the reported works related to this field and further characterization of the formed species using trimetallic carbonyl cluster of osmium is unique to this work as well.

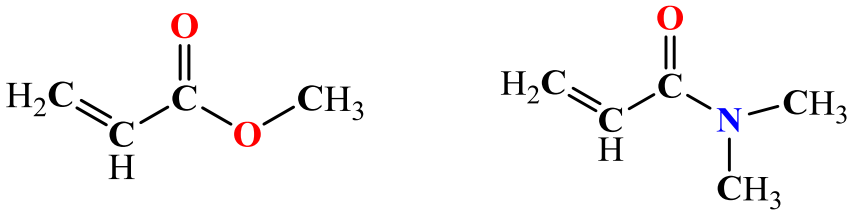

Figure 1.1 Molecular structures of MA (left) and DMA (right)

Adipic Acid, mostly derived from dimerization of MA is of high importance in industrial research and chemical manufacturing. It is primarily used for preparation of nylon, and polyurethanes, and other polymers. Its industrial synthesis involves mixture of nitric acid, cyclohexanone, and cyclohexanol which produces nitrous oxide as a byproduct and damages the ozone layer by increasing the greenhouse effect.

Numerous studies have been carried out in the past several decades to utilize transition metals as means to improve the green chemistry of adipic acid synthesis and also facilitate its preparation. Most catalytic processes employed in the chemical industry involves C6 feedstock, whereas utilizing transition metals as means to facilitate this catalytic process has facilitated usage of C3 feedstocks such as methyl acrylate as well which are cheaper and result in fewer side products.

Selective tail-to-tail coupling of olefins such as acrylates has been of interest since several decades ago because it facilitates the polymerization of such olefins. For example, dimerization of methyl acrylate has been studied in order to synthesize adipic acid and its usage as an intermediate step in pharmaceutical applications pertaining to drug synthesis. There are numerous reports of transition metal catalyzed dimerization of methyl acrylate using ruthenium[5], rhodium[6], and palladium[7].

Another way of achieving Nylon 6,6 or similar polymers is by end to end dimerization of Acrylamides such as DMA studied in this work. Achieving longer chain valuable dimers or polymers such as adipic acid or nylon 6,6 is very significant in chemical industry as it eliminates the need for mixture of different organic precursors to achieve the desired product which might include a large amount of the starting material left in the mixture after the formation of the desired product.

Numerous studies have been carried out throughout the years in order to optimize activation and end to end dimerization of MA using transition metal clusters. In the work by Barlow et al., it was found that palladium catalysts are highly selective in doing so, but they suffer from short life cycle due to precipitation.

However, McKinney et al. utilized Ru(III) complexes to catalyze dimerization of MA with assistance of Zinc and other reagents.[8]

In their proposed mechanism, C-H activation of MA Beta-carbon by ruthenium metal was assumed which was followed by insertion of another MA molecule in the Ru-H bond. Hauptman et al studied Rh (III) catalyzed dimerization of MA and proposed

initiation of the catalytic cycle by protonation of the catalyst ($Cp^*Rh(C_2H_4)_2$(Cp^* =C_5Me_5) which would subsequently react with MA[9].

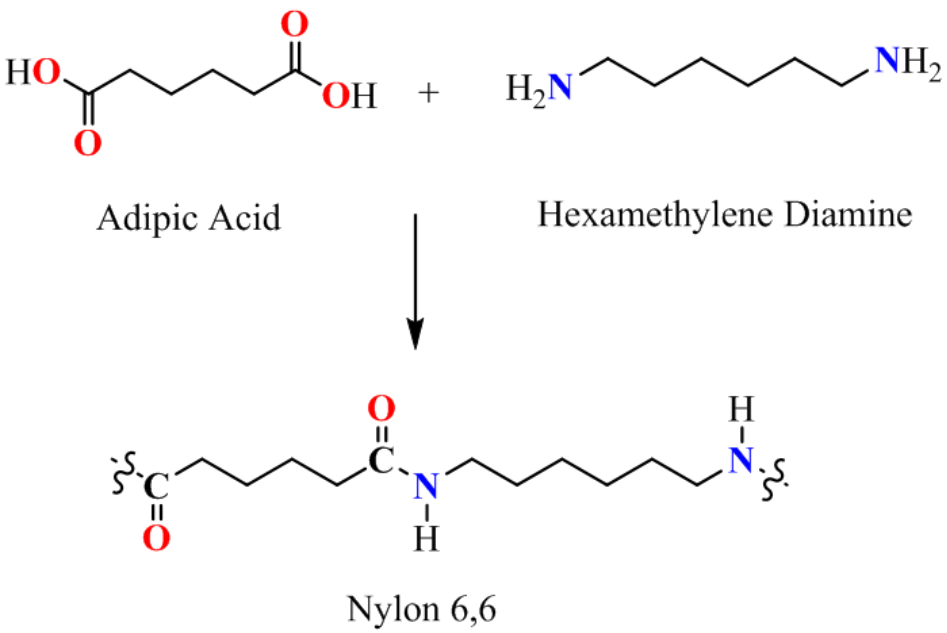

Figure 1.2 Nylon 6,6 synthesis pathway from Adipic Acid and Hexamethylene Diamine

Studies by Adams et al. have shown that multinuclear clusters of Ruthenium $Ru_5(\mu_5\text{-}C)(CO)_{15}$ can successfully activate MA's CH bond at the beta-carbon atom of the vinyl group in a oxidation addition of MA and decarbonylation of the Ru_5 cluster.

In this study, the Ru_5 cluster was treated with methyl acrylate at 80 ^{o}C to yield a coordinated CO to one of the ruthenium atoms and an open Ru_5 cluster. Then, through CO elimination, the β-hydrogen of the MA ligand was activated resulting in a chelating acrlyloyl and a 5-membered ring including one ruthenium atom formation.

All ruthenium atoms in this activated cluster follow the 18 electron rule. In addition, they have shown several alkenyl CH activation complexes of various olefins such as

dimethylformamide, vinyl acetate, N, N-dimethylacrylamide using the Ru_5C carbonyl cluster.[10] (Figure 1.3)

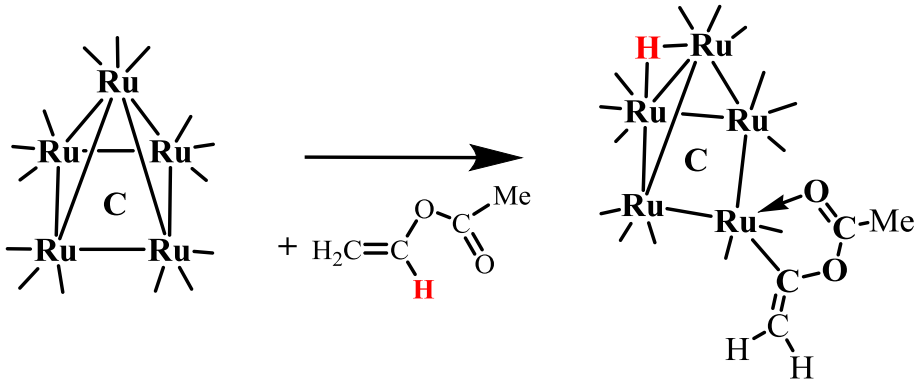

Figure 1.3 Activation of Methyl Acrylate by the $Ru_5(\mu_5\text{-}C)(CO)_{15}$ complex by Adams et al.

$Ru_5(\mu_5\text{-}C)(CO)_{15}$ was shown to activate methyl acrylate and vinyl acetate through a ring opening process in the Ru_5 cluster which enables C-H activation of the olefin by acquiring two electrons from the ligand. Both C-H activations occurred at the vinyl site of the olefins, however, at the α-carbon atom for vinyl acetate and at the beta carbon atom for methyl acrylate, respectively. This is a perfect example of substituent-directed CH activation on olefins leading to C-H activation and functionalization[11].

In a similar work by Adams et al., vinyl acetate was activated and transformed to other valuable chemicals using the previously reported binuclear rhenium complex of $Re_2(CO)_8(\mu\text{-}C_6H_5)(\mu\text{-}H)$. In this work, the dirhenium complex activates the β-carbon of methyl acrylate and the vinyl ligand is chelated to the cluster by a $\mu\text{-}\eta^2\text{-}(\sigma + \pi)$-coordinated C_2H_3 (vinyl) coordination. An interesting fact about this C-H activation is the absence of need for loss of any CO from the cluster or cleavage of any Re-Re bond unlike that of the Ru_5 cluster with methyl acrylate[12]. (Figure 1.4)

This work was an inspiration for us to attempt at activation of β-carbon of DMA and its functionalization. $Ru_5(\mu_5\text{-}C)(CO)_{15}$ becomes activated by a ring opening process which makes it suitable for oxidative addition reaction, and, similarly, $Os_3(CO)_{10}(NCCH_3)_2$ becomes activated by readily losing two acetonitrile molecules which also makes it suitable for C-H activation reactions.

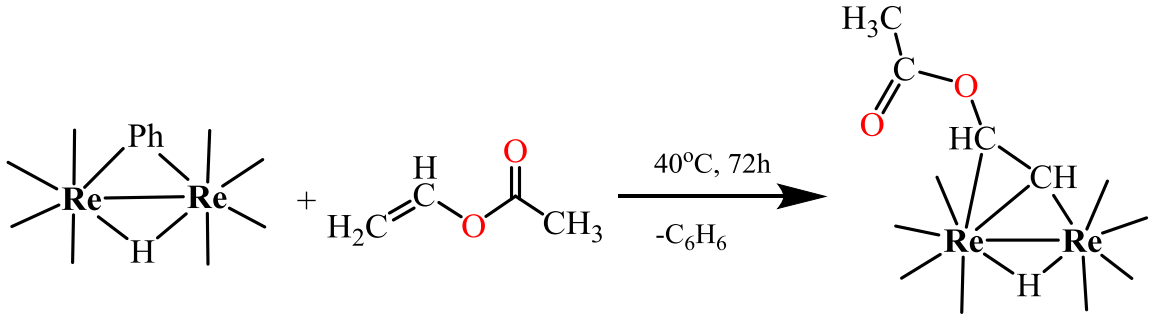

Figure 1.4 Activation of vinyl acetate by $Re_2(CO)_8(\mu\text{-}C_6H_5)(\mu\text{-}H)$ Complex by Adams et al.

This work was an inspiration for us to attempt at activation of β-carbon of DMA and its functionalization. $Ru_5(\mu_5\text{-}C)(CO)_{15}$ becomes activated by a ring opening process which makes it suitable for oxidative addition reaction, and, similarly, $Os_3(CO)_{10}(NCCH_3)_2$ becomes activated by readily losing two acetonitrile molecules which also makes it suitable for C-H activation reactions.

Osmium carbonyl clusters form stable products and through further decarbonylation by additives such as trimethylamine N-oxide, they may react with other species and transform into higher or lower nuclearity clusters. End to end dimerization of DMA may not be feasible with usage of $Ru_5(\mu_5\text{-}C)(CO)_{15}$ due to steric issues, but easily possible with Os_3 clusters as cleavage of Os-Os bond is fairly easy and the cluster can

become open and form a linear or angular configuration to facilitate the location of DMA dimer.

1.2 Experimental details

General Data. Reagent grade solvents were dried by the standard procedures and were freshly distilled prior to use. All reactions were performed under a nitrogen atmosphere. Infrared spectra were recorded on a Thermo Nicolet Avatar 360 FT-IR spectrophotometer. ^{1}H NMR and ^{31}P NMR spectra were recorded on a Varian Mercury 300 spectrometer operating at 300.1 MHz. Mass spectrometric (MS) measurements performed by a direct-exposure probe using electron impact ionization (EI) were made on a VG 70S instrument, positive/negative ion mass spectra were recorded on a Micromass Q-TOF instrument by using electrospray (ES) ionization. $Os_3(CO)_{12}$ was obtained from STREM and were used without further purification. $Os_3(CO)_{10}(NCCH_3)_2$[13] was prepared according to the previously reported procedures. Product isolations were performed by TLC in air on Analtech 0.50mm silica gel 60 Å F254 glass plates and Analtech 0.25 mm aluminum oxide UV_{254} glass plates.

Synthesis of $Os_2(CO)_6(\mu\text{-}H)(\mu\text{-}O{=}C(N(CH_3)_2)CHCH)$, 1, $Os_4(CO)_{12}(\mu\text{-}O{=}C(N(CH_3)_2)CHCH)_2$, 2, and, $Os_3(CO)_9(\mu\text{-}O{=}C(N(CH_3)_2)\ CH_2CHCCHC(N(CH_3)_2){=}O)$, 3.

$Os_3(CO)_{10}(NCCH_3)_2$ (80 mg, 0.085 mmol) were added to a 100 mL three neck flask containing a solution of N,N-dimethylacrylamide (42.50 mg, 0.428 mmol) in 60 mL heptane. The reaction mixture was allowed to stir in reflux for 7 h with intermittent monitoring by IR spectroscopy. The solvent was then removed *in vacuo*, and the product was isolated by TLC by using a mixture of hexane and methylene chloride (3:1 ratio) solvent to yield three bands. In order of elution they gave 13.1 mg of yellow $Os_2(CO)_6(\mu$-

H)(μ-O=C($N(CH_3)_2$)CHCH), **1** (16.3 % yield), 12.3 mg of $Os_4(CO)_{12}$(μ-O=C($N(CH_3)_2$)CHCH)$_2$, **2** (15.4 % yield), 23.0 mg of yellow $Os_3(CO)_9$(μ-O=C($N(CH_3)_2$)CH_2CHCCHC($N(CH_3)_2$)=O), **3** (28.8 % yield). Spectral data for **1**: IR ν_{CO} (cm^{-1} in methylene chloride): 2095(m), 2048(vs), 2011(m), 1997(s), 1975(m), 1956(m). ^{1}H NMR (CD_2Cl_2, 25°C, TMS, in ppm) δ = -12.77 (s, 1H, Hydride), δ = 5.32 (s,1H, CH), δ = 6.58 (s,1H, CH), δ = 3.54 (s, 6H, $N(CH_3)_2$); Mass Spec. Pos. Ion ES/MS *m*/*z* 649. Spectral data for **2**: IR ν CO (cm^{-1} in methylene chloride): 2093 (w), 2085(w), 2069(s), 2047(m), 2034(m), 1998(s), 1978(m). ^{1}H NMR (CD_2Cl_2, 25°C, TMS, in ppm) δ = 11.94 (d, 2H, CH), 11.14 (s, 6H, $N(CH_3)_2$), 8.18 (d, 2H, CH). Mass Spec. EI+/MS *m*/*z*= 1295 (M^+). Spectral data for **3**: IR ν CO (cm^{-1} in methylene chloride): 2121 (w), 2070(m), 2059(s), 2048(vs), 2005(s), 1982(s), 1962(s), 1935(w). ^{1}H NMR (CD_2Cl_2, 25°C, TMS, in ppm) δ = 8.01 (d, 1H, CH_2), 7.61 (t, 1H, CH), 4.69 (d, 1H, CH_2, 3.62 (s, 6H, $N(CH_3)_2$). Mass Spec. EI+/MS *m*/*z*= 1020 (M^+).

Synthesis of $Os_3(CO)_8$(μ-O=C($N(CH_3)_2$)CHCH)$_2$, 4, and $Os_6(CO)_{20}$(μ-H)(μ-O=C($N(CH_3)_2$)CHCH)$_2$, 5.

$Os_3(CO)_{10}(NCCH_3)_2$ (80 mg, 0.085 mmol) were added to a 100 mL three neck flask containing a solution of N,N-dimethylacrylamide (144.3 mg, 1.45 mmol) in 60 mL methylene chloride. The reaction mixture was allowed to stir at reflux for 12 h with intermittent monitoring by IR spectroscopy. The solvent was then removed *in vacuo*, and the product was isolated by TLC by using a mixture of hexane and methylene chloride (3:1 ratio) solvent to yield two bands. In order of elution they gave 5.0 mg of yellow $Os_3(CO)_8$ (μ-O=C($N(CH_3)_2$)CHCH)$_2$, **4** (6.2 % yield), 18.2 mg of $Os_6(CO)_{20}$(μ-H)(μ-O=C($N(CH_3)_2$)CHCH)$_2$, **5** (22.5 % yield). Spectral data for **4**: IR ν_{CO} (cm^{-1} in methylene

chloride): 2094(w), 2077(m), 2068(m), 2059(vs), 2034(w), 2004(m), 1989(s), 1967(m).^{1}H NMR (CD_2Cl_2, 25^{o}C, TMS, in ppm) δ = 7.98 (d,2H, CH), δ = 7.5 (d, 2H, CH), δ = 3.54 (s, 6H, $N(CH_3)_2$); Mass Spec. Pos. Ion ES/MS *m*/*z* = 984. Spectral data for **5**: IR ν CO (cm^{-1} in methylene chloride): 2124 (w), 2085(s), 2074(m), 2060(w), 2050(m), 2040(vs), 2018(w), 2007(w), 1988(w). ^{1}H NMR (CD_2Cl_2, 25^{o}C, TMS, in ppm) δ = -13.94 (s, Hydride), δ = 8.45 (d, 1H, CH), 4.82 (d, 1H, CH), 3.05 (s, 3H, $N(CH_3)_2$), 2.72 (s, 3H, $N(CH_3)_2$). Mass Spec. EI+/MS *m*/*z*= 1802 (M^+).

Synthesis of $HOs_3(CO)_{10}$(μ-O=C(N$(CH_3)_2$)CHCH), 6.

$Os_3(CO)_{10}(NCCH_3)_2$ (80 mg, 0.085 mmol) were added to a 100 mL three neck flask containing a solution of N,N-dimethylacrylamide (192.4 mg, 1.94 mmol) in 30 mL methylene chloride. The reaction mixture was allowed to stir at room temperature for 2 h with intermittent monitoring by IR spectroscopy. The solvent was then removed *in vacuo*, and the product was isolated by TLC by using a mixture of hexane and methylene chloride (1:1 ratio) solvent to yield three bands. In order of elution they gave 5.0 mg of yellow known compound Os_3 $(CO)_{11}$(μ-H)(μ-Cl) (6.42 % yield), 6.1 mg of yellow known compounds $Os_3(CO)_{12}$(μ-H)(μ-OH), (8.00 % yield), 55.8 mg of yellow $Os_3(CO)_9$(μ-H)(μ-O=C(OCH_3)CHCH), **6** (69.11 % yield). Spectral data for **6**: IR ν_{CO} (cm^{-1} in methylene chloride): 2110(w), 2074(s), 2045(w), 2017(s), 1980(m).^{1}H NMR (CD_2Cl_2, 25^{o}C, TMS, in ppm) δ = -9.831 (s, 1H, Hydride), δ = 8.36 (s,1H, CH), δ = 4.62 (s,1H, CH), δ = 2.96 (s, 6H, $N(CH_3)_2$); Mass Spec. Pos. Ion ES/MS *m*/*z* = 910.

Synthesis of $Os_5(CO)_{15}(\mu\text{-}O{=}C(N(CH_3)_2)CHCH)_2$, 7.

$HOs_3(CO)_{10}$ (μ-O=C(N$(CH_3)_2$)CHCH), **6** (30 mg, 0.032 mmol) was added to a NMR tube containing a solution of trimethylamine N-oxide (4.0 mg, 0.04 mmol) in 3 mL d-methylene chloride. The reaction mixture was placed in oil bath at 45 °C for 7 days with intermittent monitoring by NMR spectroscopy. The solvent was then removed by evaporation at room temperature, and the product was isolated by TLC by using a mixture of hexane and methylene chloride (1:1 ratio) solvent to yield three bands. In order of elution they gave 3.0 mg of yellow $Os_3(CO)_{12}$, (10.34 % yield), 5 mg of $Os_2(CO)_6(\mu\text{-}H)(\mu\text{-}O{=}C(N(CH_3)_2)CHCH)$, **1** (24.13% yield), and 10.2 mg of $Os_5(CO)_{15}(\mu\text{-}O{=}C(N(CH_3)_2)CHCH)_2$, **7** (20.71% yield). Spectral data for **7**: IR ν_{CO} (cm^{-1} in methylene chloride): 2091(w), 2071(m), 2056(s), 2015(m), 1990(s).^{1}H NMR (CD_2Cl_2, 25°C, TMS, in ppm) δ = -15.03 (s, 1H, Hydride), δ = 5.68 (s,1H, CH), δ = 5.02 (s,1H, CH), δ = 2.887(s, 6H, N$(CH_3)_2$); Mass Spec. EI+/MS *m*/*z*= 1802 (M^+).

Synthesis of $Os_3(CO)_9(\mu\text{-}H)(\mu\text{-}O{=}C(OCH_3)CHCH)$, 8.

$Os_3(CO)_{10}(NCCH_3)_2$ (80 mg, 0.085 mmol) were added to a 100 mL three neck flask containing a solution of methyl acrylate ($CH_3OCOCHCH_2$) (36.91 mg, 0.42 mmol) in 60 mL hexane. The reaction mixture was allowed to stir in reflux for 3 h with intermittent monitoring by IR spectroscopy. The solvent was then removed *in vacuo*, and the product was isolated by TLC by using a mixture of hexane and methylene chloride (3:1 ratio) solvent to yield three bands. In order of elution they gave 5.0 mg of yellow known compound $Os_3(CO)_{11}(\mu\text{-}H)(\mu\text{-}Cl)$ (6.25 % yield), 6.1 mg of yellow known compounds $Os_3(CO)_{12}(\mu\text{-}H)(\mu\text{-}OH)$, (7.63 % yield), 23 mg of yellow $Os_3(CO)_9(\mu\text{-}H)(\mu\text{-}O{=}C(OCH_3)$

CHCH), **8** (28.75 % yield). Spectral data for **8**: IR ν_{CO} (cm^{-1} in methylene chloride): 2096(w), 2068(s), 2037(vs), 2009(s), 1997(m).^{1}H NMR (CD_2Cl_2, 25°C, TMS, in ppm) δ = -13.94 (s, 1H, Hydride), δ = 9.084 (d, 1H, CH), δ = 5.54 (d, 1H, CH), δ = 3.52 (s, 3H, OCH_3); Mass Spec. Pos. Ion ES/MS *m*/*z* = 910.

1.3 Crystallographic Analyses

Yellow crystals of **1**, **2**, **3**, **4**, **6**, **7**, **8** and red single crystals of **5** suitable for x-ray diffraction analyses were obtained by slow evaporation of solvent from solutions in hexane/methylene chloride solvent mixtures at 5 °C. Each crystal was glued onto the end of a thin glass fiber. X-ray intensity data were measured by using a Bruker SMART APEX CCD-based diffractometer using Mo Kα radiation (λ = 0.71073 Å). The raw data frames were integrated with the SAINT+ program by using a narrow-frame integration algorithm.[14] Corrections for Lorentz and polarization effects were also applied by using SAINT+.

An empirical absorption correction based on the multiple measurement of equivalent reflections was applied by using the program SADABS. All structures were solved by a combination of direct methods and difference Fourier syntheses, and refined by full-matrix least-squares on F^2 by using the SHELXTL software package.[15] All non-hydrogen atoms were refined with anisotropic displacement parameters. Hydrogen atoms were placed in geometrically idealized positions and included as standard riding atoms during the final cycles of least-squares refinement.

Crystal data, data collection parameters, and results of the analyses are listed in Tables 1.1, 1.2, and 1.3. Compounds **1**, **3**, and **7** crystallized in the triclinic crystal system.

The space group $P\bar{1}$ was assumed for both **1**, **3** and **7** was confirmed by the successful solution and refinement for the structure in each case. Compound **2** crystallized in the orthorhombic crystal system and the space group Pna2(1) was identified by the systematic absences in the diffraction data. Compounds **4**, **5**, **6**, and **8** crystallized in the monoclinic crystal system. For compound **4,** the space group C2/c, for compound **5** space group Cc, for compound **6**, space group C(2)/c, and for compound **8** space group P2(1)/c were identified by the systematic absences in the diffraction data.

1.4 Results and Discussion

N,N-dimethylacrylamide (DMA) has a formula of $(CH_3)_2NC(=O)CHCH_2$ and is a clear, colorless to yellowish liquid with a boiling point of 171.0 ºC and density of 0.964 $g.cm^{-3}$. DMA is an unsaturated amide which contains one α and two β hydrogens and a double bond between α and β carbon atoms. (Figure 1.1)

$Os_3(CO)_{10}(NCCH_3)_2$ is a useful activated form of $Os_3(CO)_{12}$ which was reported in 1981 by Johnson et al [13]. It can be easily made by reaction of $Os_3(CO)_{12}$ with trimethylamine N-oxide in a mixture of methylene chloride and acetonitrile at room temperature for 2 hours in almost 100% yield.

In the reactions of $Os_3(CO)_{10}(NCCH_3)_2$ with DMA, seven CH-activated compounds were obtained, and they are all shown in Scheme 1.1. The carbonyl ligands coordinated to the osmium atoms are not shown for clarity. The products of this reaction include one Os_2, three Os_3, one Os_4, one Os_5 and one Os_6 clusters containing activated DMA. Among the activated DMA complexes, **1**, **5**, and **7** contain bridging hydrides and compound **6** contains a terminal hydride ligand bonded to the osmium atom not coordinated

by activated DMA. Compounds **2**, **3**, **4**, and **7** contain two activated DMA ligands in their structure which is in the form of an acryloyl in **2**, **4**, and **7** and in the form of a dimer in **3**All of the compounds are electronically saturated clusters which all meet the requirements of the 18 electron rule.

In order to show how $Os_3(CO)_{12}$ was transformed into the products, we propose the mechanism outlined in scheme 1.2. The carbonyl ligands coordinated to osmium atoms were omitted for clarity. As mentioned earlier in synthesis of the DMA activated products, $Os_3(CO)_{10}(NCCH_3)_2$, a decarbonylated form of $Os_3(CO)_{12}$, was used in reaction with DMA molecule because it readily loses two acetonitrile molecules in the solution or in reaction with another molecule and becomes unsaturated by four electrons which makes the triosmium cluster much more reactive and suitable for C-H activation and oxidative addition reactions.

As is outlined in scheme 1.2, upon interaction with decarbonylated osmium metal atoms, it is expected that the oxygen atom in the carbonyl group of DMA approaches the osmium atom first, binds to the metal atom, and acts as a directing group which brings the remainder of the transition metal closer to the rest of the molecule and provides the grounds for activation of α– and β–hydrogen atoms on the vinyl group (**I_a**).

Once DMA approaches the activated Os_3 cluster, we propose that its vinyl group (C_2H_3) coordinates to the osmium atom previously approached by the oxygen atom of DMA (**I_b**). The intermediate through which the transition metal forms a bond with the β–hydrogen atom is proposed to form a six-membered ring including Os-O-C-C-C-H which eases the access of transition metal to the β–hydrogen atom and its ultimate activation and

is favorable and more stable compared to the five-membered ring intermediate for activation of α-hydrogen.

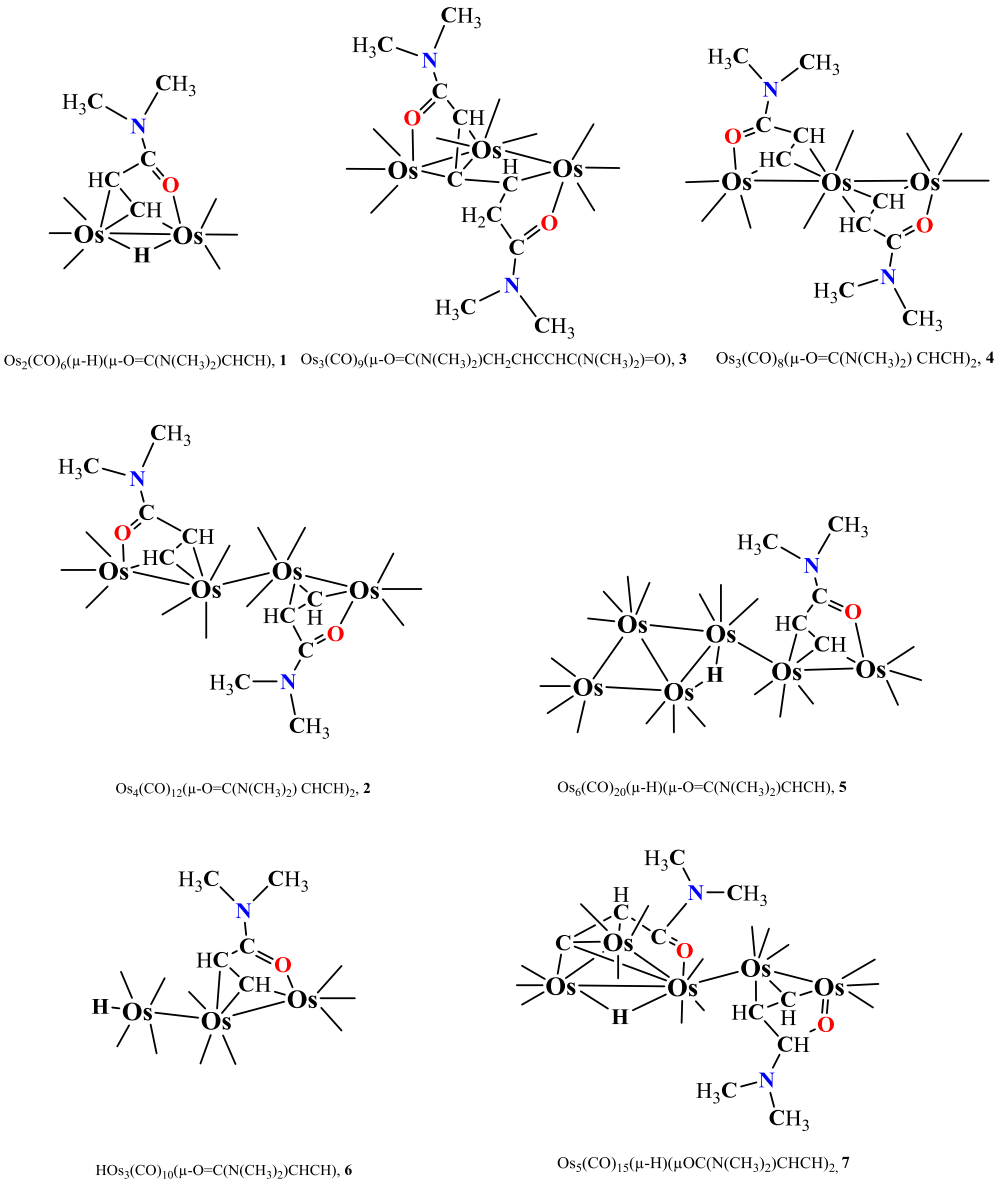

Scheme 1.1. Line structures of seven CH-activated osmium cluster compounds obtained from reactions of $Os_3(CO)_{10}(NCCH_3)_2$ and DMA: $Os_2(CO)_6(\mu\text{-}H)(\mu\text{-}O{=}C(N(CH_3)_2)CHCH)$, **1**, $Os_4(CO)_{12}(\mu\text{-}O{=}C(N(CH_3)_2CHCH)_2$, **2**, and, $Os_3(CO)_9(\mu\text{-}O{=}C(N(CH_3)_2)CH_2CHCCHC(N(CH_3)_2){=}O)$, **3**, $Os_3(CO)_8(\mu\text{-}O{=}C(N(CH_3)_2)CHCH)_2$, **4**, $Os_6(CO)_{20}(\mu\text{-}H)(\mu\text{-}O{=}C(N(CH_3)_2)CHCH)_2$, **5**, $HOs_3(CO)_{10}(\mu\text{-}O{=}C(N(CH_3)_2)CHCH)$, **6**, and $Os_5(CO)_{15}(\mu\text{-}H)(\mu\text{-}O{=}C(N(CH_3)_2)CHCH)_2$, **7**.

Because of the presence of the double bond between α- and β– carbons of DMA, vinyl segment of DMA coordinates to the cluster through a μ-η^2-($\sigma + \pi$)-coordinated vinyl coordination which similar to acryloyl coordination found in vinyl acetate activation by $Re_2(CO)_8(\mu\text{-}C_6H_5)(\mu\text{-}H)$ studied by Adams et al. In this process, β- carbon forms a σ bond and α and β–carbon atoms form a π- coordination to the Os_3 cluster.

Compound **6** is formed by coordination of oxygen atom to the cluster, cleavage of Os-Os bond and upon activation of β–hydrogen of chelated DMA. It is a saturated 50 electron complex and is a significant step in synthesis of all the obtained species in this study since **6** is a precursor to majority of the identified complexes. It is crucial to note that in **6** the hydride ligand is not a bridge between two osmiums in the cluster but is instead a terminally-coordinated hydride ligand. In addition, the osmium atom containing the hydride ligand has four carbonyl groups coordinated to it whereas the other two osmium atoms have only three (Figure 1.11)

This means if this osmium atom loses a CO then the cluster becomes unsaturated with this linear configuration, therefore there would be a need for formation of Os-Os bond so that the cluster becomes closed and the saturation requirement become 48 instead of 50, making it possible for the complex to become saturated by forming this metal-metal bond which results in a saturated 48 electron species, $\mathbf{I^*}$ (Figure 1.5). $\mathbf{I_c}$ is an intermediate through which the transformation occurs through which terminal hydride forms a bridge between two osmium atoms and Os-Os forms.

We made numerous attempts to decarbonylate **6** using trimethylamine N-oxide to isolate $\mathbf{I^*}$, however, all those attempts were unsuccessful. As outlined in figure 1.5, $\mathbf{I^*}$

contains an acryroyl bridging (μ_3-) between all three osmium atoms and a bridging hydride (μ_2-) unlike **6**. The equivalent of **I*** was isolated by reaction of $Os_3(CO)_{10}(NCCH_3)_2$ with MA yielding **8** (Figure 1.13). Because of the significant similarity between **I*** and **8**, we expect them to have very similar characterizations such as the hydride NMR resonance, and IR absorption spectrum.

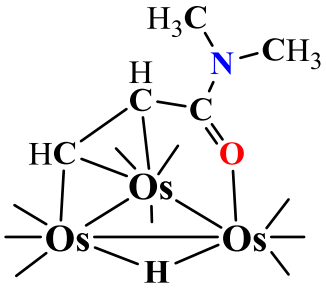

Figure 1.5. Proposed structure of **I***, a saturated 48 e species with the formula of $Os_3(CO)_9(\mu\text{-}H)(\mu_3\text{-}O{=}C(N(CH_3)_2)CHCH)$.

Compounds **1**, **2**, and **3** were formed as a result of 1:5 reaction between $Os_3(CO)_{10}(NCCH_3)_2$ and DMA in reflux of heptane for 7 hours.

Figure 1.6 shows an ORTEP diagram of the molecular structure of $Os_2(CO)_6(\mu\text{-}H)(\mu\text{-}O{=}C(N(CH_3)_2)CHCH)$, **1**, showing 30% thermal ellipsoid probability. Compound **1** is a 34 electron saturated species which includes a bridging acryroyl (μ_2-) between Os1 and Os2 in which O1 is coordinated to Os2 with a bond length of 2.120(3) Å and Os1-Os2 bond length of 2.8997(3) Å. Bridging hydride (μ-H) ligand forms a 1.85(6) Å bond to Os1 and a 1.69(6) Å bond to Os2. The difference between the bond length between Os1-H1 and Os2-H1 can be justified by the asymmetrical geometry of the vinyl coordination to Os_2 cluster. Atoms C2 and C3 of the chelated vinyl group are coordinated through a $\mu\text{-}\eta^2\text{-}(\sigma$ +

π) coordination to the Os_2 cluster unlike O1-Os2 bond which causes an imbalance in the symmetry of the formed bonds between Os1-H1 and Os2-H1.

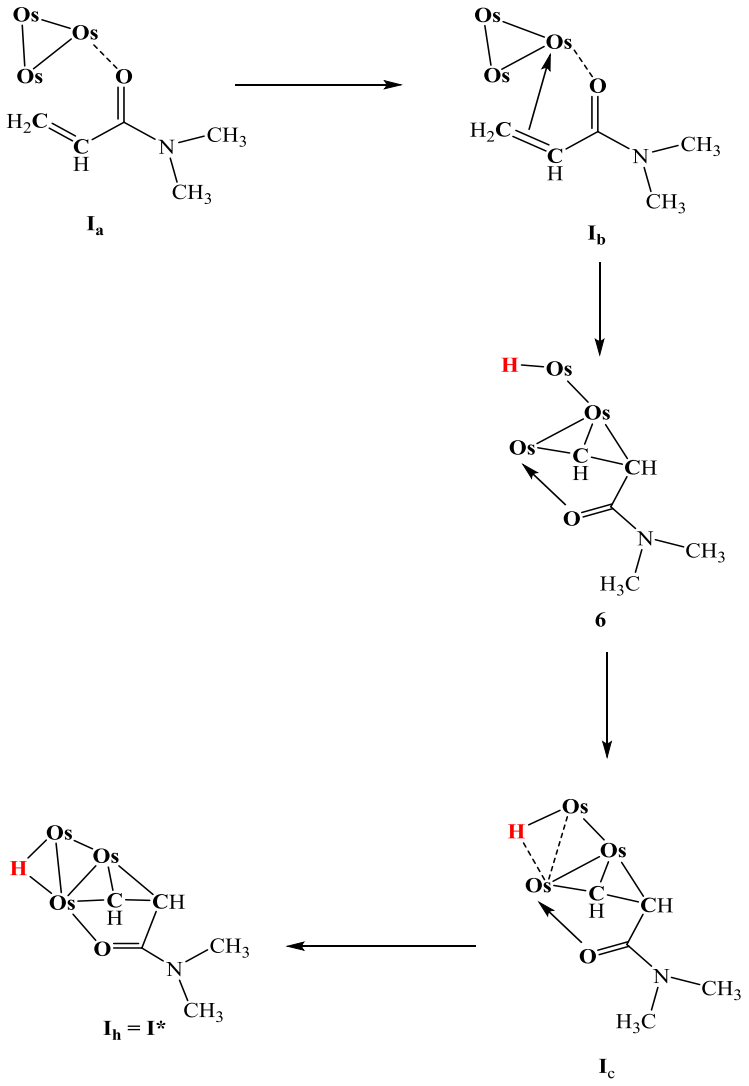

Scheme 1.2. Proposed mechanism of C-H activation of DMA by triosmium carbonyl cluster and formation of **I*** and **6**.

Compound **2** is a 66 electron complex which is also an electronically saturated structure. There are no bridging hydride (μ-H) ligands in this complex, however, there are two activated DMA molecules in the form of bridging acryloyls between Os1-Os2 and Os3-Os4. The Os2-Os3 bond is slightly longer that Os1-Os2 and Os3-Os4 which is

perfectly reasonable as there is no chelated DMA molecule bridging between them and causing them to become close to one another. On the other hand, Os1-Os2 has almost the same bond length as Os3-Os4 since they both are bridged by identical acryloyl groups. (Figure 1.7)

As is the case with **2**, compound **3** also does not have any bridging hydride ligands in its structure and no hydride NMR resonances were observed either (Figure 1.8). Compound **3** is a 50 electron saturated complex which satisfies the 18 electron rule for each metal atom in the complex.

As mentioned earlier in this work, **3** contains a dimer between two DMA molecules chelated to the Os_3 cluster through ($\sigma + \pi$) coordination to the Os2 and σ coordination to Os3 and Os1. This is a perfect example of end to end dimerization of DMA using polynuclear transition metal clusters which to our knowledge has not been studied before.

As it will be discussed later in this chapter, we propose that **3** was formed by treatment of **6** with excess DMA through a transformation process outlined in scheme 1.4 which involves C-C coupling between the β-carbon atoms of each DMA molecule and additional CH activation of the β-hydrogen of DMA. However, we propose that once the second DMA molecule is activated by the cluster, the first and the second bridging hydride ligands are reductively eliminated by formation of a molecule of H_2.

The Os1-Os2 bond length is about 2.8394(3) Å and Os2 – Os3 bond length is about 2.9025(3) Å which demonstrates that the former is slightly shorter. This can be explained by coordination of C3, C2, and O1, which are considered to be on the left hand side of the cluster, to Os2 whereas only C4 and O2 coordination to the right hand side of it which

creates an asymmetrical configuration with more atoms bridging between Os1-Os2 than Os2-Os3.

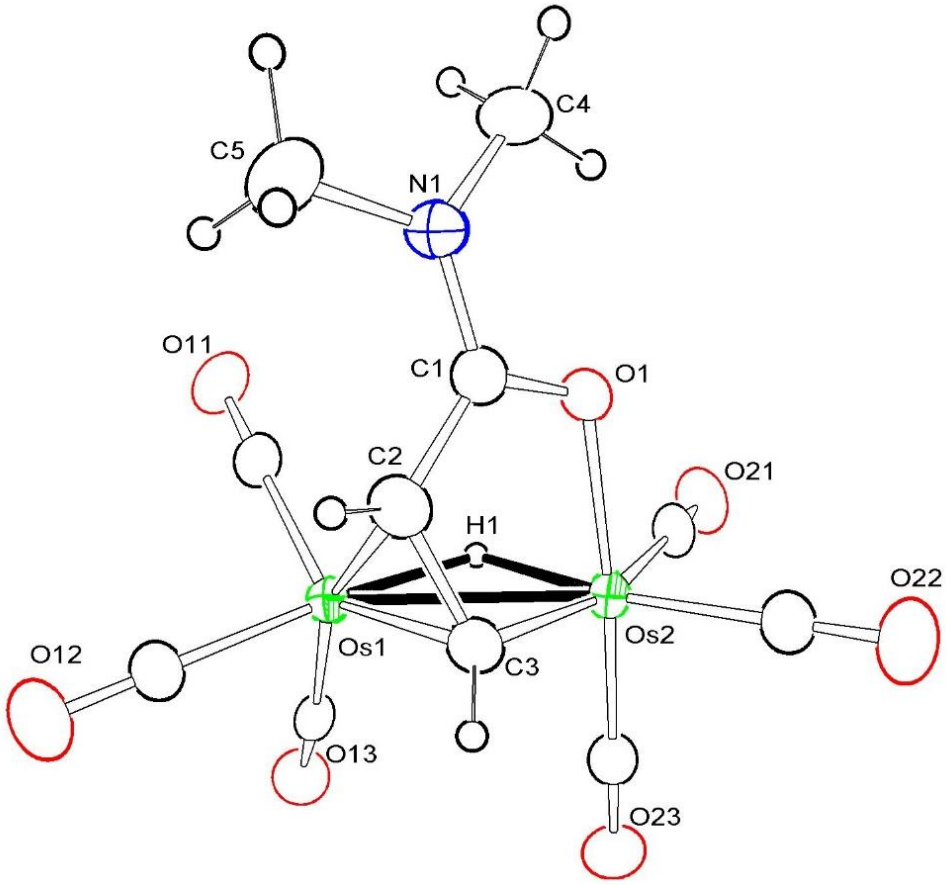

Figure 1.6 ORTEP diagram of the molecular structure of, $Os_2(CO)_6(\mu\text{-}H)(\mu\text{-}O{=}C(N(CH_3)_2)CHCH)$, **1**, showing 30% thermal ellipsoid probability. Selected interatomic bond distances (Å) and angles (º) are as follow: Os(1) – Os(2) = 2.8997(3), Os(2) – O(1) = 2.120(3), Os(1) – C(3) = 2.137(5), Os(2) – C(3) = 2.080 (5), Os(1) – C(2) = 2.210 (4), Os(1) – H(1) = 1.85 (6), Os(2) – H(1) = 1.69 (6), C3 – Os1– H1= 78.3(17), Os2 – Os1– H1 = 33.0(17), Os1– Os2– H1= 36.6

Compounds **4** and **5** were formed as a result of 1:2 reaction between $Os_3(CO)_{10}(NCCH_3)_2$ and DMA in reflux of methylene chloride for 12 hours. Compound **4** has a similar structure to **3** and, as we propose in scheme 1.4, we expect that it actually was formed by decarbonylation of **3**.

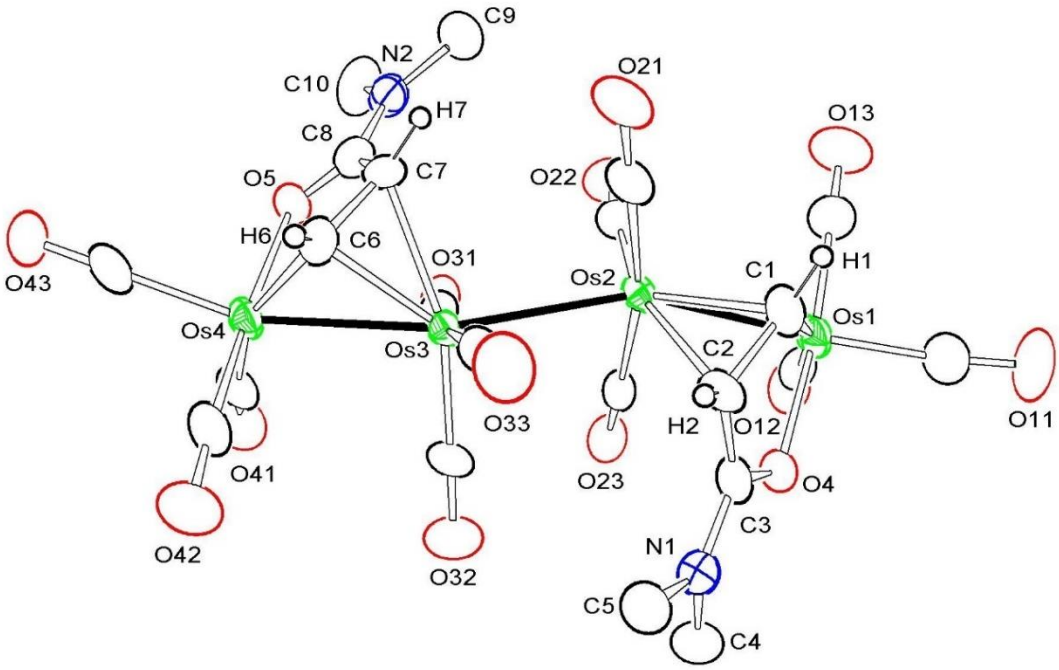

Figure 1.7 ORTEP diagram of the molecular structure of**,** $Os_4(CO)_{12}(\mu\text{-}O{=}C(N(CH_3)_2)CHCH)_2$, **2**, showing 30% thermal ellipsoid probability. Selected interatomic bond distances (Å) and angles (°) are as follow: Os(1) – Os(2) = 2.8271(5), Os(2) – Os(3) = 2.8826(4), Os(4) – Os(3) = 2.8173(5), Os(1) – C(1) = 2.010(10), Os(2) – C(1) = 2.215(9), Os(3) – C(6) = 2.200(9), Os(4) – C(6) = 2.022(10), Os(1) – O(4) = 2.129(6), Os(4) – O(5) = 2.123(5); C(1) – Os(1) – Os(2) = 51.2(3), C(2) – Os(2) – Os(1) = 68.4(2), C(2) – Os(2) – Os(3) = 99.3(2), Os(1) – Os(2) – Os(3) = 157.218(16).

However, there is no DMA-DMA dimer in **4** and both α- and β- carbons of each DMA are coordinated to Os2, forming two chelated acryloyl groups bridging between $Os1^i$ and $Os2^i$ as well as Os1 and Os2. (Figure 1.9) Due to the symmetry of the complex, it is expected that the bond length between $Os1^i$-Os2 and Os1-Os2 to be identical and bond length of 2.82678(19) Å proves this assertion.

However, there is not a DMA-DMA dimer in **4** and both α- and β- carbons of each DMA is coordinated to Os2, forming two chelated acryloyls bridging between $Os1^i$ and Os2 as well as Os1 and Os2. (Figure 1.9)

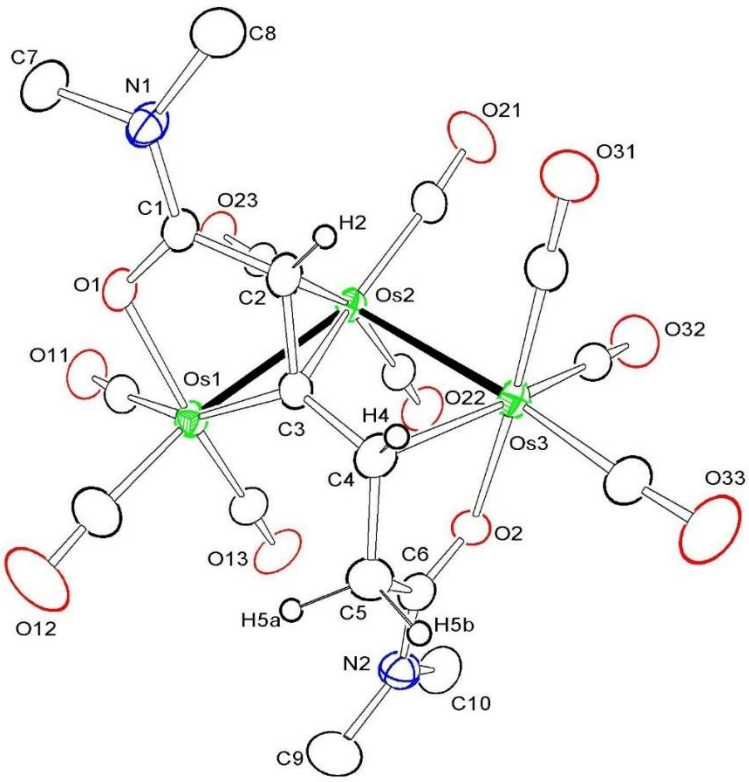

Figure 1.8 ORTEP diagram of the molecular structure of**,** $Os_3(CO)_9(\mu\text{-}O{=}C(N(CH_3)_2)CH_2CHCCHC(N(CH_3)_2){=}O)$, **3**, showing 30% thermal ellipsoid probability. Selected interatomic bond distances (Å) and angles (º) are as follow: Os(1) – Os(2) = 2.8394(3), Os(2) – Os(3) = 2.9025(3), Os(1) – C(3) = 2.093(4), Os(1) – O(1) = 2.130(3), Os(2) – C(1) = 1.895(5), Os(3) – C(4) = 2.181(5), Os(3) – O(2) = 2.131(3), C(3) – C(4) = 1.476(6); O(1) – Os(1) – Os(2) = 83.13(9), Os(1) – Os(2) – Os(3) = 104.141(8), C(3) – C(4) – Os(3) = 100.5(3).

Due to the symmetry of the complex, it is expected that the bond length between $Os1^{i}$-Os2 and Os1-Os2 to be identical and bond length of 2.82678(19) Å proves this assertion.

Moreover, compound **5** is the only Os_6 complex identified and characterized in this work and it has an interesting unopened Os_3 carbonyl fragment bonded to an open Os_3 fragment which contains a bridging acryrolyl between Os5-Os6 (Figure 1.10). As we will propose later in this work, we assume synthesis of **5** by reaction between **6** and $Os_3(CO)_{12}$

which undergoes Os-Os formation and decarbonylation of both terminal osmium of **6** and one of osmium atoms in $Os_3(CO)_{12}$ (Scheme 1.6).

In compound **5**, Os1-Os2 bond length of 2.8053(4) Å is significantly shorter than Os4-Os5 bond length of 2.8800(4) Å which can easily be explained by existence of a closed Os1-Os2-Os3 trimetallic ring which causes the Os-Os bond length to be shorter compared to that of Os4-Os5. In addition, the Os5-Os6 bond, although not included in a triosmium ring, is also significantly shorter that Os4-Os5 which can be due to existence of a bridging acryloyl between Os5 and Os6 which contributes to shortness of the Os4-Os5 bond length.

Compound **6** was formed from the reaction between $Os_3(CO)_{10}(NCCH_3)_2$ and DMA at room temperature in methylene chloride in 1 hour. As it will be illustrated in scheme 1.7, it is a crucial isolated complex which we propose to be an intermediate to synthesis and formation of majority of the identified compounds. It is a saturated 50 electron species for a configuration of its type and contains a bridging acryloyl ligand between Os1-Os2 in addition to a terminal hydride H3 (Figure 1.11).

On the other hand, compound **7** was formed by reaction of **6** with trimethylamine N-oxide at 45°C in methylene chloride in 7 days. Since we predicted the existence of $\mathbf{I}^*$, decarbonylation of **6** was an attempt to synthesize and isolate it since in order for the cluster of **6** to be transformed into a closed Os_3 cluster, by removal of a CO ligand from the terminal osmium atom and formation of a Os-Os bond was required (Scheme 1.2).

However, the unexpected isolation of **7** was achieved which we believe occurred through an unknown mechanism either through first formation of $\mathbf{I}^*$ and additional Os-Os

bond formation or through transformations in the structure of **6** after the decarbonylation step.

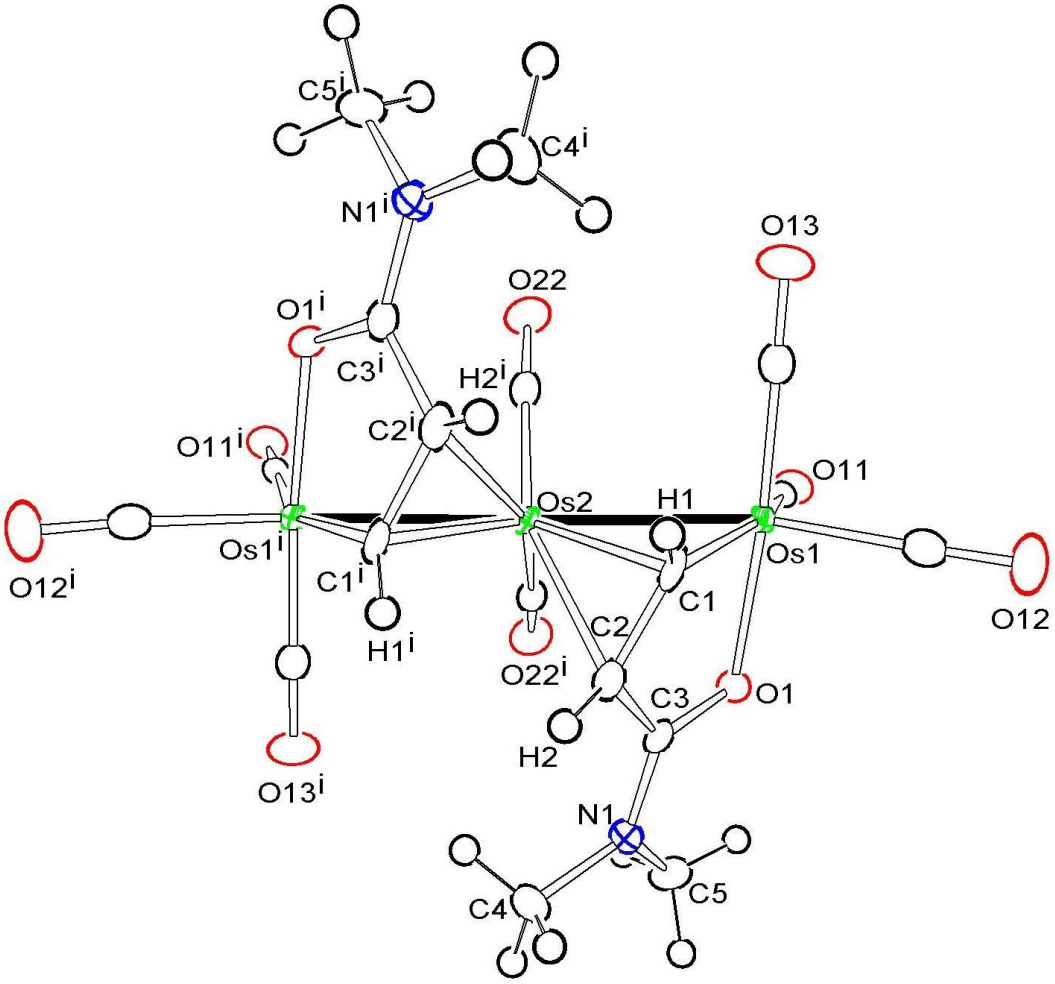

Figure 1.9 ORTEP diagram of the molecular structure of, $Os_3(CO)_8(\mu\text{-}O{=}C(N(CH_3)_2)CHCH)_2$, **4**, showing 30% thermal ellipsoid probability. Selected interatomic bond distances (Å) and angles (°) are as follow: Os(1) – Os(2) = 2.82678(19), Os(2) – Os(1^i) = 2.82678(19), Os(1) – C(1) = 2.031(4), Os(1) – O(1) = 2.129(3); C(1) – Os(2) – C(1^i) = 94.5(2), Os(1) – Os(2) – Os(1^i) = 174.946(9), Os(1) – C(1) – Os(2) = 83.74(14), O(1) – Os(1) – Os(2) = 82.43(7).

We believe either of the aforementioned processes could result in formation of **7**. Compound **7** contains a triply bridged (μ_3-) acryloyl group bonded to Os3, Os4, and Os5 (Figure 1.12) which is very similar to the structure proposed to exist in **I*** and a (μ_2-) acryloyl bridge between Os1-Os2 which exists in **6**. The bond length between Os1-Os2 in

7 is very close to that of **6** (Os1-Os2: 2.8111(4)) which is expected as they both are similar fragments containing the same olefin as a bridge.

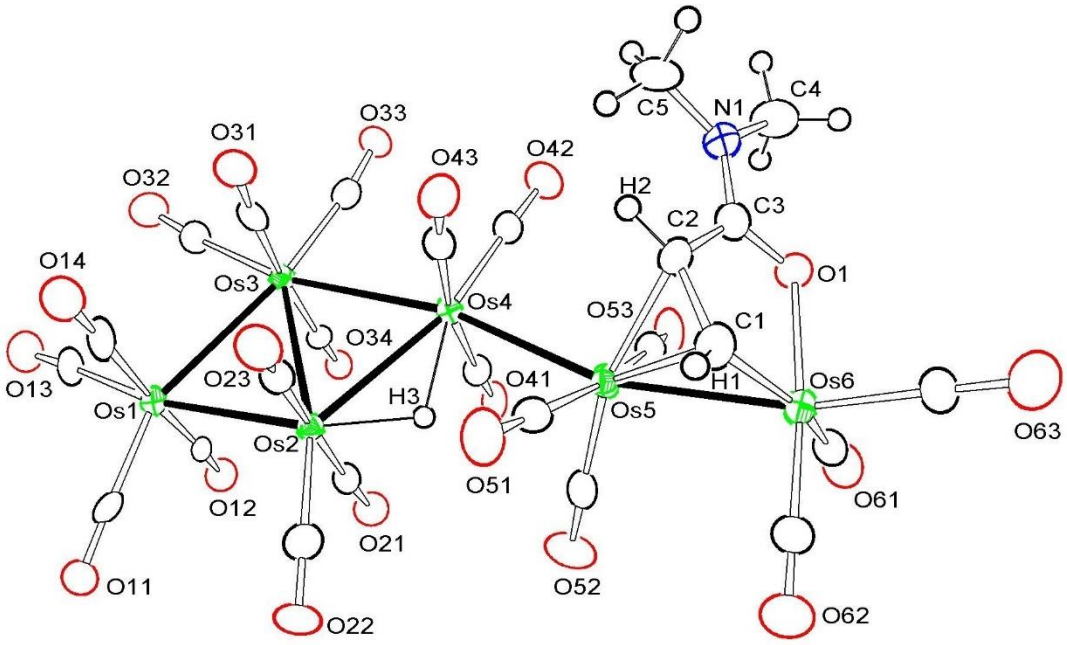

Figure 1.10 ORTEP diagram of the molecular structure of, $Os_6(CO)_{20}(\mu\text{-}H)(\mu\text{-}O{=}C(N(CH_3)_2)CHCH)$, **5**, showing 30% thermal ellipsoid probability. Selected interatomic bond distances (Å) and angles (°) are as follow: Os(1) – Os(2) = 2.8053(4), Os(2) – Os(3) = 2.9134(4), Os(2) – Os(4) = 2.9162(4), Os(4) – Os(5) = 2.8800(4), Os(5) – Os(6) = 2.8272(4), Os(4) – H(3) = 1.86(9), Os(2) – H(3) = 1.78(8), Os(5) – C(2) = 2.289(8), Os(6) – O(1) = 2.135(5), Os(6) – C(1) = 2.057(8); Os(1) – Os(2) – Os(3) = 62.086(10), Os(1) – Os(2) – Os(4) = 124.414(12), Os(3) – Os(2) – Os(4) = 124.414(12), Os(6) – Os(5) – Os(4) = 159.684(14).

The formation of **6** is the most important step in synthesis of all the acquired complexes in this work as it acts as a precursor to almost all of the other compounds. Upon treatment of $Os_3(CO)_{10}(NCCH_3)_2$ with excess DMA in methylene chloride, compound **6** forms at room temperature through and oxidative addition process and upon heating the reaction mixture it transforms directly to **1**, **3**, and **5**. One of the most interesting of these transformations is the cleavage of Os-Os bond and a shift in the terminal hydride to a bridging hydride between two of the other osmium atoms.

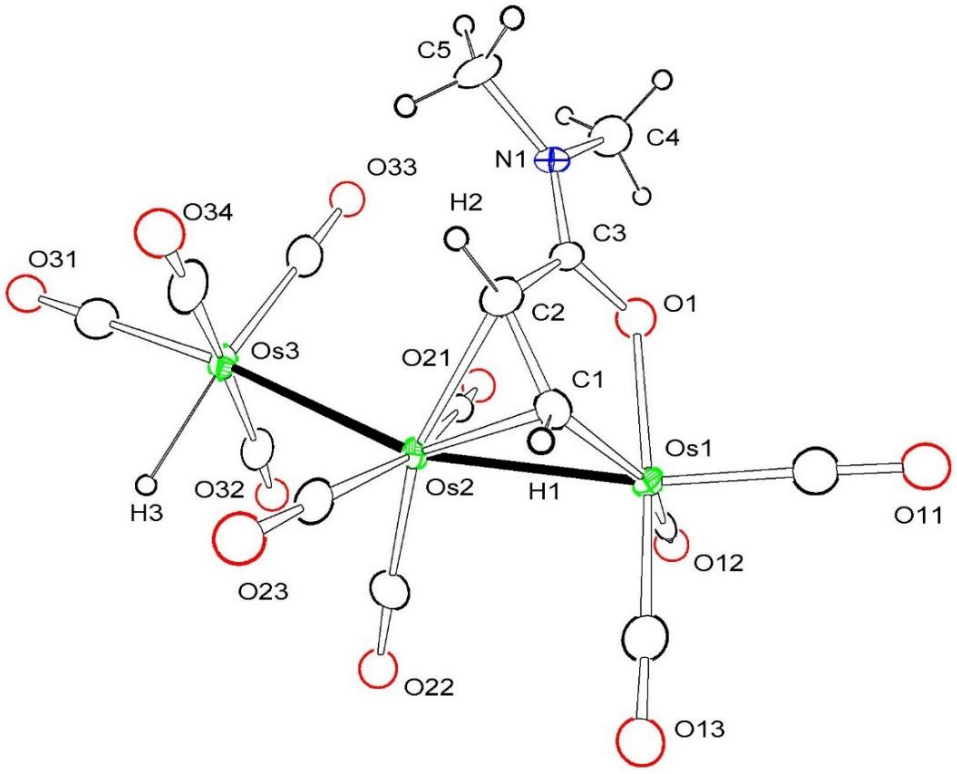

Figure 1.11 ORTEP diagram of the molecular structure of $HOs_3(CO)_{10}(\mu$-$O{=}C(N(CH_3)_2)CHCH)$, **6**, showing 30% thermal ellipsoid probability. Selected interatomic bond distances (Å) and angles (°) are as follow: Os(1) – Os(2) = 2.8154(3), 2.8930(4), Os(3) – H(3) = 1.89(6), 2.020(6), Os(2) – C(1) = 2.215(9), Os(2) – C(2) = 2.294(6), Os(1) – O(1) = 2.126(4), Os(1) – C(1) = 2.020(6); C(13) – Os(1) – Os(2) = 91.72(19), O(1) – Os(1) – Os(2) = 82.13(10), Os(2) – Os(3) – H(3) = 83.3(18), Os(1) – Os(2) – Os(3) = 157.352(11).

Scheme 1.3 depicts the proposed mechanism of transformation of **6** to **1** at high temperatures. We propose that **6**, a saturated 50 electron species, cleaves an Os-Os bond resulting in formation of binuclear **1** and $Os(CO)_4$**.** Compound **1** is a saturated 34 electron cluster and is stable at room temperature. In addition, hydride shifts from the terminal hydride onto the other two neighboring osmium atoms. In addition, we propose that **6** is transformed to **3** upon treatment with excess DMA and heat through a process in which the terminal hydride in the former shifts onto the bridging carbon of the chelating DMA and

another DMA molecule couples with it to form a C-C bond while the yielding dimer is still chelated to the cluster forming **3**, a 48 electron saturated complex

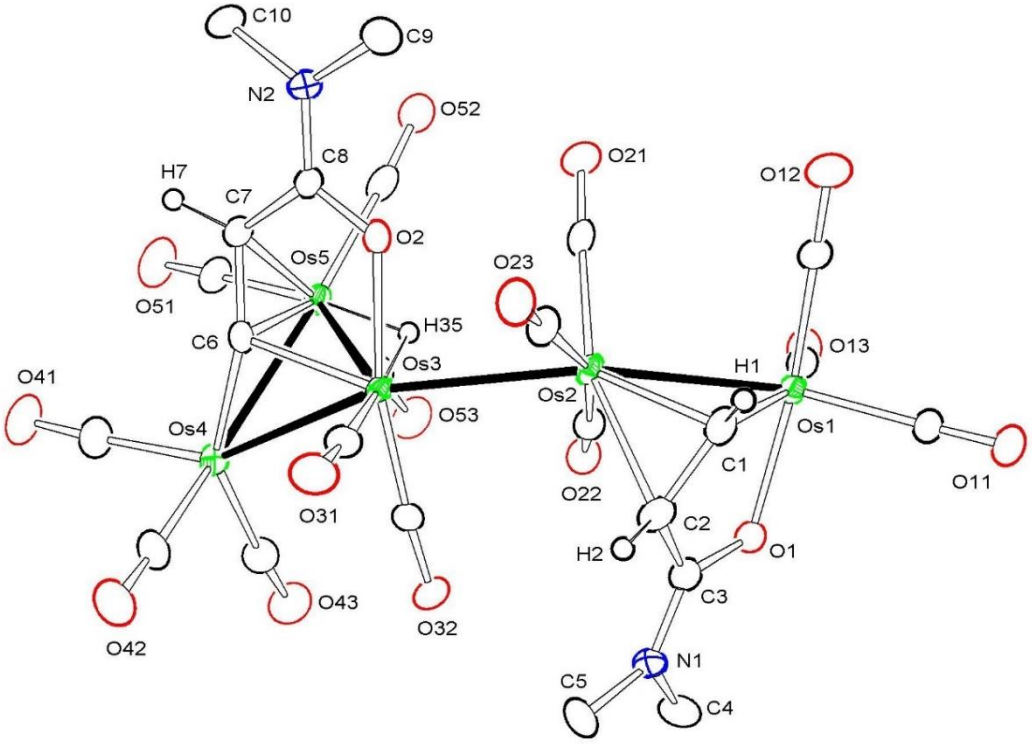

Figure 1.12 ORTEP diagram of the molecular structure of, $Os_5(CO)_{15}(\mu\text{-}O{=}C(N(CH_3)_2)CHCH)_2$, **7**, showing 30% thermal ellipsoid probability. Selected interatomic bond distances (Å) and angles (º) are as follow: Os(1) – Os(2) = 2.8111(4), Os(2) – Os(3) = 2.8563(4), Os(4) – Os(3) = 2.8635(4), Os(5) – Os(4) = 2.8460(4), Os(1) – C(1) = 2.040(7), Os(2) – C(1) = 2.171(7), Os(3) – C(6) = 2.088(6), Os(4) – C(6) = 1.926(7), Os(1) – O(1) = 2.121(5), Os(3) – O(2) = 2.143(5); C(1) – Os(1) – O (1) = 2.143(5), C(1) – Os(2) – C(2) = 37.6(3), C(1) – Os(1) – Os(2) = 50.14(19), Os(1) – Os(2) – Os(3) = 159.706(13).

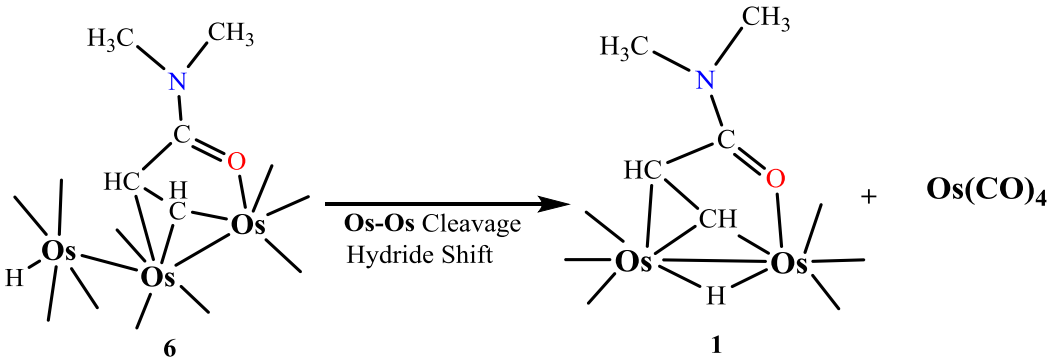

Scheme 1.3. Proposed scheme for transformation of **6** to **1**.

In this reaction, coupling of two DMA molecules assisted by trimetallic complex of osmium was achieved. In order to fully saturate the cluster, the formed dimer undergoes H_2 elimination so the μ_3 carbon can donate three electrons to the cluster instead of two resulting in a saturated 48 electron complex **3**. Scheme 1.4 shows the proposed mechanism of conversion of **6** to **3**. In **3**, there is one μ_3 and one μ_2 bridging carbon atoms.

Furthermore, as shown in scheme 1.5, through an interesting process of hydrogen shift within the chelated dimer, we propose that **3** transforms to **4** by involvement of α-carbon of one of the dimer's carbonyls in forming a metal-carbon bond. In this process, the previously μ_3 carbon atom in **3** becomes μ_2 and the newly involved α-carbon, which previously possessed two hydrogen atoms, transfers one of its hydrogen atoms to the former μ_3 carbon resulting in two μ_2 carbons.

We also propose that **5** is formed by addition of $Os_3(CO)_{12}$ to **6** in a process through which two Os-Os bonds are formed between the terminal Osmium of **6** and two osmium atoms of $Os_3(CO)_{12}$. The terminal hydride ligand in **6** becomes μ_2 between terminal osmium of **6** and one of the osmium atoms in $Os_3(CO)_{12}$.

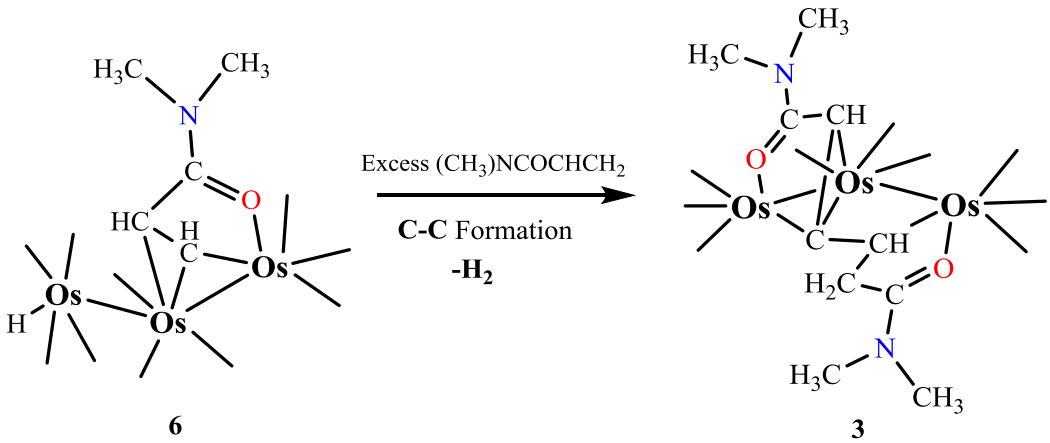

6 **3**

Scheme 1.4. Proposed scheme for transformation of **6** to **3**.

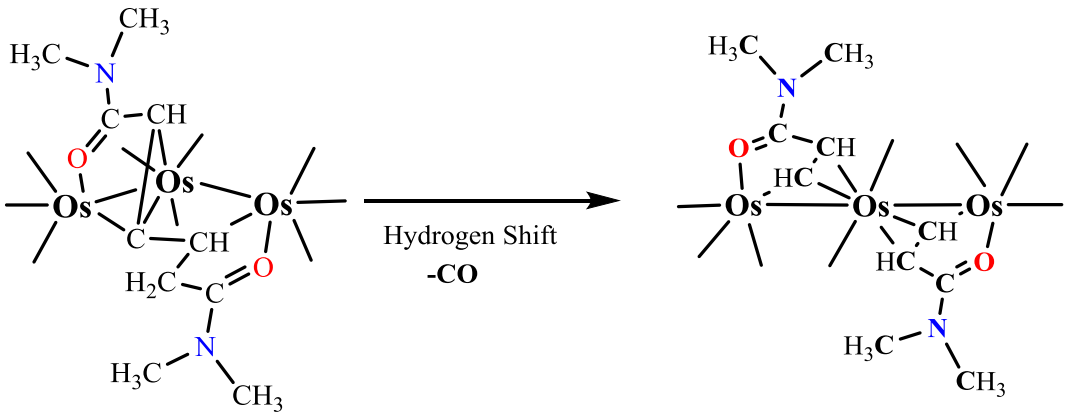

3 4

Scheme 1.5. Proposed scheme for transformation of **3** to **4**.

In order to yield a stable saturated complex, two CO ligands were eliminated, one of them from the terminal osmium of **6** and one from one of osmiums in $Os_3(CO)_{12}$, yielding **5** which is a saturated 94 electron cluster. Proposed scheme of formation of **5** from **6** is shown in scheme 1.6.

Through another Os-Os formation process, we propose that **1** is transformed at high temperature through a reductive elimination of H_2 to yield **2**. Scheme 1.7. illustrates conversion of **1** to **2**.

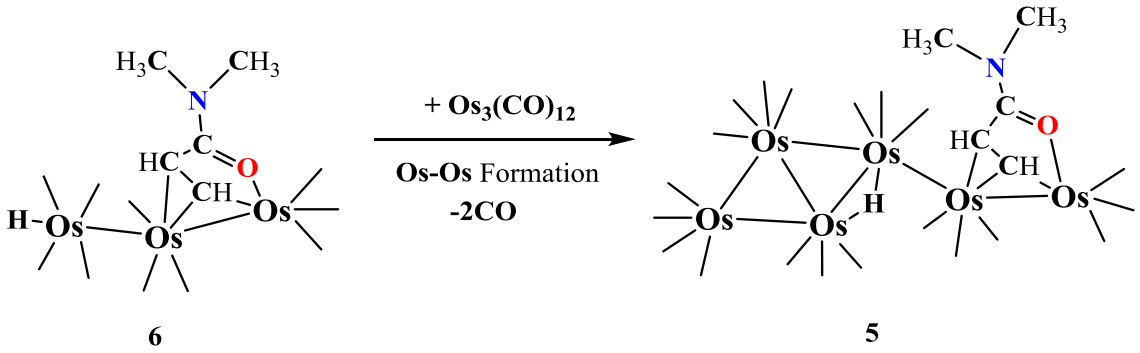

6 5

Scheme 1.6. Proposed scheme for transformation of **6** to **5**.

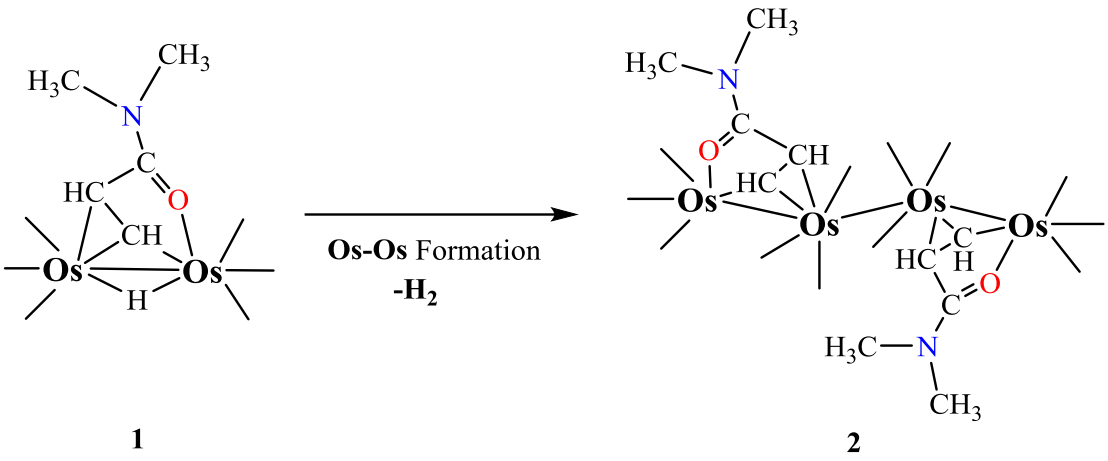

Scheme 1.7. Proposed scheme for transformation of **1** to **2**.

Although we were not able to isolate and characterize **I***, reaction of $Os_3(CO)_{10}(NCMe)_2$ with methyl acrylate yielded **8** which is triple bridging chelating methyl acrylate on the trisomium cluster. We propose existence of **I*** which has the same electron count and same chelating vinyl group as in **8**. However, as mentioned earlier in this study, we believe that **6** is a precursor to synthesis of other species characterized in this study and not **8**. Proposed mechanism for formation of **6** and its transformation to **I*** was discussed earlier in scheme 1.2.

In addition, compound **8** was formed by reaction of $Os_3(CO)_{10}(NCCH_3)_2$ with MA in reflux of hexane for 3 hours. Compound **8** is a 48 electron saturated closed cluster with a triply bridged acryloyl (μ_3-C_2H_2) group coordinated to all the osmium atoms in the cluster in addition to a bridging hydride (μ-H) ligand (Figure 1.13).

As mentioned earlier in this work, compound **8** is an ester equivalent of **I*** with a -OCH_3 fragment bonded to the carbonyl's carbon atom of the acryloyl instead of a –$N(CH_3)_2$ group. Compound **8** was easily isolated and identified without any need for further decarbonylation of Os_3 cluster.

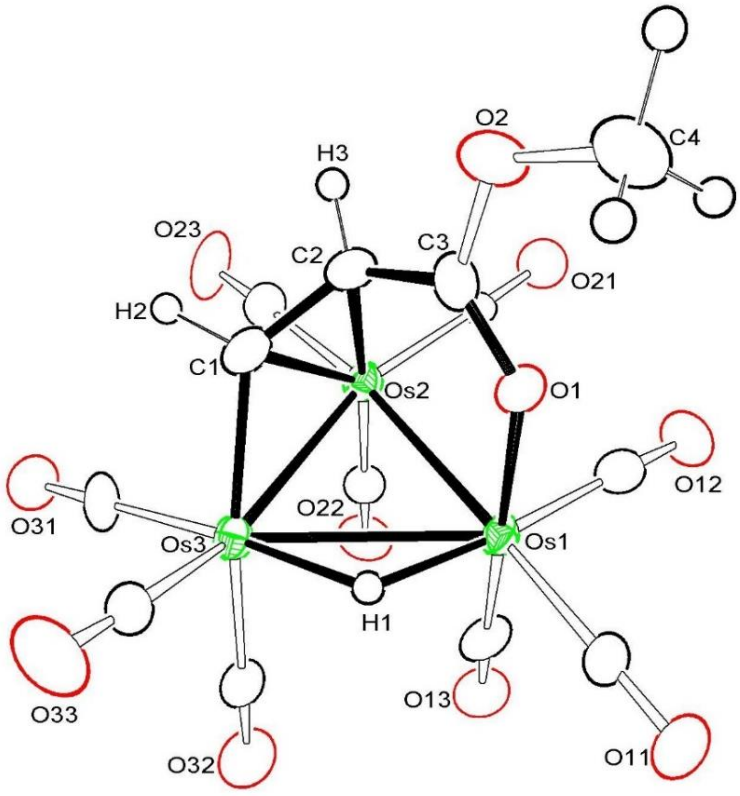

Figure 1.13 ORTEP diagram of the molecular structure of, $Os_3(CO)_9(\mu\text{-}H)(\mu\text{-}O{=}C(OCH_3)CHCH)$, **8**, showing 30% thermal ellipsoid probability. Selected interatomic bond distances (Å) and angles (°) are as follow: Os(1) – Os(2) = 2.8398(6), Os(1) – Os(3) = 2.9636(6), Os(2) – Os(3) = 2.8091(6), Os(1) – H(1) = 1.80(2), Os(3) – H(1) = 1.80(2), Os(1) – O(1) = 2.130(7), Os(3) – C(1) = 2.069(11); Os(2) – Os(1) – Os(3) = 57.852(15), Os(2) – Os(1) – H(1) = 90.6(12), Os(3) – Os(1) – H(1) = 34.7(7).

It is expected that **I*** would have very similar bond lengths and bond angles to **8** as they both are very similar in structure. The bond length between Os1-Os2 is very similar to Os2-Os3 and they both are significantly shorter than that of Os1-Os3 which can be explained by existence of a C1-C2 bridge on the edge of Os2-Os3 and C2-C3-O1 on the edge of Os1-Os2 whereas existence of merely a bridging hydride on the edge of Os1-Os3.

The mechanism through which **8** is formed is unknown since there is no other activated MA complex identified to aid us in explaining the reaction process, but considering it was formed in a 28% yield shows that it was synthesized by direct C-H

activation and μ_3 coordination to the Os_3 cluster and not from any other precursors unlike what we expect would be the case with **I***.

1.5 Summary and Conclusions

In this study, the activation of the C-H bond on the β-carbon of methyl acrylate and N,N-dimethyl acrylamide using a trimetallic carbonyl cluster of osmium was studied and further transformations resulting from this C-H activation and their resulting interesting species were isolated and characterized.

In this work, various species with different nuclearity of osmium were isolated, a chelating dimer of DMA was formed, transformations of trisomium cluster to each of the other characterized species were proposed, and existence of a missing complex (**I***) was predicted. In addition, an ester equivalent of **I*** was isolated and characterized in which methyl acrylate was used to react with activated Os_3 cluster instead of N,N-dimethyl acrylamide.

Synthesis and characterization of **6** was a crucial step in understanding the mechanism of synthesis of majority of the identified species and proposed mechanisms for transformation of **6** to **1**, **3** and **5** were studied. In addition, it was proposed that **2** and **4** were formed from **1** and **3**, respectively. Scheme 1.7 summarizes the synthesis and transformations of the characterized activated DMA chelating cluster complexes. The variety of species obtained from simple reaction of $Os_3(CO)_{10}(NCCH_3)_2$ with DMA proves the complexity of mechanism involved in synthesis of each reported complex.

This study can be further enriched by additional studies on electron density of each species using Quantum Theory of the Atom in a Molecule (QTAIM) model[16] which might confirm or reject proposed mechanisms and predictions made in this work.

In addition, considering Osmium and Ruthenium are both in group VIII of the periodic table, similar C-H activations and further transformations can be studied by using the $Ru_3(CO)_{12}$ cluster complex because it possesses the same electron count, reacts easier even without a need for activation, and forms stable clusters. Furthermore, activated cluster of methyl acrylate, **8**, can be further studied in hopes of isolating the equivalent clusters with various nuclearity studied in this work.

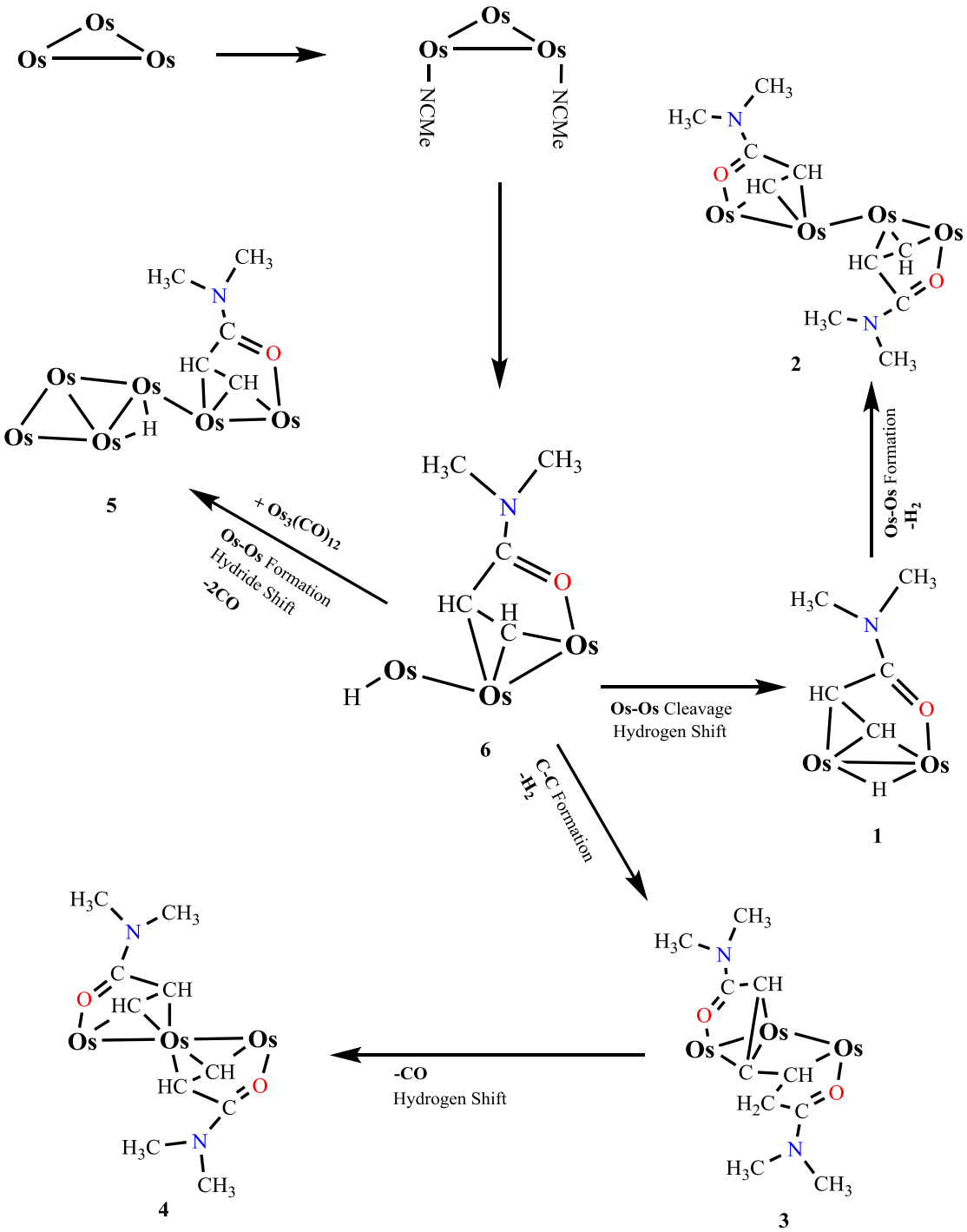

Scheme 1.8. A schematic mechanism for synthesis and transformations of **1**, **2**, **3**, **4**, **5**, and **6**.

Table 1.1 Crystallographic Data for Compounds 1, 2 and 3.

COMPOUND	**1**	**2**	**3**
Empirical formula	$Os_2NO_7H_9C_{11}$	$Os_4N_2O_{14}C_{22}H_{16}$	$Os_3N_2O_{11}C_{19}H_{16}$
Formula weight	647.65	1293.17	1018.94
Crystal system	Triclinic	Orthorhombic	Triclinic
Lattice parameters			
a (Å)	9.7387(5)	22.2594(9)	8.2350(3)
b (Å)	9.8739(5)	7.2928(3)	9.4604(3)
c (Å)	10.3898(5)	18.4471(7)	16.4609(6)
α (deg)	62.4050(10)	90.00	93.3680(10)
β (deg)	94.647(1)	90.00	91.4300(10)
γ (deg)	60.747(2)	90.00	108.9270(10)
V (Å^3)	765.97(7)	2994.6(2)	1209.66(7)
Space group	$P\ \bar{1}$	*P*na2(1)	$P\ \bar{1}$
Z value	2	4	2
ρ_{calc} (g / cm^3)	2.808	2.868	2.504
μ (Mo Kα) (mm^{-1})	16.601	16.985	7.081
Temperature (K)	302(2)	302(2)	294(2)
$2\Theta_{max}$ (°)	59.9	55.2	55.94
No. Obs. ($I > 2\sigma(I)$)	5091	5249	12496
No. Parameters	205	389	1123
Goodness of fit (GOF)	1.044	1.106	0.978
Max. shift in cycle	0.002	0.003	0.001
Residuals*: R_1; wR_2	0.0535; 0.1430	0.0357; 0.0677	0.0449; 0.0865
Absorption Correction,	Multi-scan	Multi-scan	Multi-scan
Max/min	0.1283 / 0.0326	1.000 / 0.2677	1.000 / 0.4749
Largest peak in Final	2.927	1.618	1.861
Diff. Map (e$^-$ / Å^3)			

*$R_1 = \Sigma_{hkl}(||F_{obs}| - |F_{calc}||)/\Sigma_{hkl}|F_{obs}|$; $wR_2 = [\Sigma_{hkl}w(|F_{obs}| - |F_{calc}|)^2/\Sigma_{hkl}wF^2_{obs}]^{1/2}$; $w = 1/\sigma^2(F_{obs})$; GOF = $[\Sigma_{hkl}w(|F_{obs}| - |F_{calc}|)^2/(n_{data} - n_{vari})]^{1/2}$.

Table 1.2 Crystallographic Data for Compounds 4, 5 and 6.

COMPOUND	**4**	**5**	**6**
Empirical formula	$Os_3N_2O_{10}H_8C_{18}$	$Os_6NO_{21}C_{25}H_9$	$Os_3NO_{11}H_9C_{15}$
Formula weight	982.86	1800.53	949.83
Crystal system	Monoclinic	Monoclinic	Monoclinic
Lattice parameters			
a (Å)	17.0726(9)	28.3586(16)	24.2516(18)
b (Å)	6.8836(4)	8.0529(5)	13.3745(10)
c (Å)	19.3694(10)	15.8597(9)	15.5724(11)
α (deg)	90.00	90.00	90.00
β (deg)	100.141(2)	101.968(2)	126.2982(16)
γ (deg)	90.00	90.00	90.00
V (Å3)	2240.7(2)	3543.1(4)	4070.8(5)
Space group	C2/c	Cc	C2/c
Z value	4	4	8
ρcalc (g / cm3)	2.550	2.336	3.100
μ (Mo Kα) (mm-1)	7.081	7.081	18.739
Temperature (K)	294(2)	294(2)	100(2)
2Θmax (°)	52.46	54.12	55.36
No. Obs. (I > 2σ(I))	6246	5543	4471
No. Parameters	444	353	313
Goodness of fit (GOF)	1.063	1.026	1.099
Max. shift in cycle	0.000	0.019	0.001
Residuals*: R1; wR2	0.0551; 0.1513	0.0328; 0.0833	0.0281;0.0613
Absorption Correction,	Multi-scan	Multi-scan	Multi-scan
Max/min	1.000 / 0.3225	1.000 / 0.4653	1.000 / 0.6377
Largest peak in Final	2.808	2.041	1.080
Diff. Map (e- / Å3)			

*$R = \Sigma_{hkl}(\,|\,|F_{obs}|-|F_{calc}|\,|)/\Sigma_{hkl}|F_{obs}|$; $R_w = [\Sigma_{hkl}w(|F_{obs}|-|F_{calc}|)^2/\Sigma_{hkl}wF^2_{obs}]^{1/2}$; $w = 1/\sigma^2(F_{obs})$; GOF = $[\Sigma_{hkl}w(|F_{obs}|-|F_{calc}|)^2/(n_{data} - n_{vari})]^{1/2}$.

Table 1.3 Crystallographic Data for Compounds 7 and 8.

COMPOUND	**7**	**8**
Empirical formula	$Os_5N_2O_{16}H_{16}C_{24}$	$Os_3O_{11}H_6C_{13}$
Formula weight	1539.39	908.78
Crystal system	Triclinic	Monoclinic
Lattice parameters		
a (Å)	10.8152(8)	9.4989(5)
b (Å)	11.6213(8)	10.8940(5)
c (Å)	14.0818(10)	17.8101(9)
α (deg)	66.965(3)	90.00
β (deg)	82.032(3)	100.152(2)
γ (deg)	82.233(3)	90.00
V (Å3)	1606.7(2)	1814.15(16)
Space group	$P\ \bar{1}$	P2(1)/c
Z value	2	4
ρcalc (g / cm3)	2.550	1.794
μ (Mo Kα) (mm-1)	7.081	7.081
Temperature (K)	294(2)	294(2)
2Θmax (°)	52.46	55.5
No. Obs. (I > 2σ(I))	6246	4471
No. Parameters	444	313
Goodness of fit (GOF)	1.063	1.099
Max. shift in cycle	0.000	0.001
Residuals*: R1; wR2	0.0551; 0.1513	0.0281; 0.0613
Absorption Correction,	Multi-scan	Multi-scan
Max/min	1.000 / 0.3225	1.000 / 0.6377
Largest peak in Final Diff.	2.808	1.080
Map (e- / Å3)		

*$R = \Sigma_{hkl}(\,|\,|F_{obs}|-|F_{calc}|\,|)/\Sigma_{hkl}|F_{obs}|$; $R_w = [\Sigma_{hkl}w(|F_{obs}|-|F_{calc}|)^2/\Sigma_{hkl}wF^2_{obs}]^{1/2}$; $w = 1/\sigma^2(F_{obs})$; GOF = $[\Sigma_{hkl}w(|F_{obs}|-|F_{calc}|)^2/(n_{data}-n_{vari})]^{1/2}$.

1.6 References

1. Labinger, J. A.; Bercaw, J. E., Understanding and exploiting C–H bond activation. *Nature* **2002,** *417* (6888), 507.

2. Willis, M. C., Transition metal catalyzed alkene and alkyne hydroacylation. *Chemical reviews* **2009,** *110* (2), 725-748.

3. Armanino, N.; Carreira, E. M., Ruthenium-catalyzed intramolecular hydrocarbamoylation of allylic formamides: Convenient access to chiral pyrrolidones. *Journal of the American Chemical Society* **2013,** *135* (18), 6814-6817.

4. Li, B.; Park, Y.; Chang, S., Regiodivergent access to five-and six-membered benzo-fused lactams: Ru-catalyzed olefin hydrocarbamoylation. *Journal of the American Chemical Society* **2014,** *136* (3), 1125-1131.

5. Alderson, T.; Jenner, E.; Lindsey Jr, R., Olefin-to-Olefin Addition Reactions. *Journal of the American Chemical Society* **1965,** *87* (24), 5638-5645.

6. Alderson, T., E. L, Jenner, RV Lindsey, Jr. *J. Am. Chem. Soc* **1965,** *87*, 5638.

7. Zhao, A. X.; Chien, J. C., Palladium catalyzed ethylene-carbon monoxide alternating copolymerization. *Journal of Polymer Science Part A: Polymer Chemistry* **1992,** *30* (13), 2735-2747.

8. McKinney, R. J.; Colton, M. C., Homogeneous ruthenium-catalyzed acrylate dimerization. Isolation, characterization and crystal structure of the catalytic precursor bis (dimethyl muconate)(trimethyl phosphite) ruthenium (0). *Organometallics* **1986,** *5* (6), 1080-1085.

9. Hauptman, E.; Sabo-Etienne, S.; White, P. S.; Brookhart, M.; Garner, J. M.; Fagan, P. J.; Calabrese, J. C., Design and Study of Rh (III) Catalysts for the Selective Tail-to-Tail

Dimerization of Methyl Acrylate. *Journal of the American Chemical Society* **1994,** *116* (18), 8038-8060.

10. Adams, R. D.; Smith, M. D.; Tedder, J. D., Substituent-Directed Activation of CH Bonds in Activated Olefins by Ru5 (μ5-C)(CO) 15. *European Journal of Inorganic Chemistry* **2018,** *2018* (25), 2984-2986.

11. Adams, R. D.; Smith, M. D.; Tedder, J. D.; Wakdikar, N. D., Selective Activation of CH Bonds in Polar Vinyl Olefins and Coupling of Ethylene to the Activated Carbon Atoms in Pentaruthenium Complexes. *Inorganic Chemistry* **2019,** *58* (13), 8357-8368.

12. Adams, R. D.; Dhull, P.; Kaushal, M.; Smith, M. D., The activation and transformations of vinyl acetate at a dirhenium carbonyl center. *Journal of Organometallic Chemistry* **2019**, 120969.

13. Johnson, B. F. G.; Lewis, J.; Pippard, D. A., The preparation, characterisation, and some reactions of [Os3(CO)11-(NCMe)]. *Journal of the Chemical Society, Dalton Transactions* **1981,** (2), 407-412.

14. *SAINT*$^{+}$, 6.2a; Bruker Analytical X-ray Systems Inc. : Madison, WI, 2001.

15. Sheldrick, G. M. *SHELTXTL*, 6.1; Bruker Analytical X-ray Systems In. : Madison, WI, 1997.

16. Cortés-Guzmán, F.; Bader, R. F., Complementarity of QTAIM and MO theory in the study of bonding in donor–acceptor complexes. *Coordination Chemistry Reviews* **2005,** *249* (5-6), 633-662.